

Interior Dynamics of Hairy Black Holes

Rong-Gen Cai
Institute of Theoretical Physics
Chinese Academy of Sciences
Ningbo University

Refs: RGC, L.Li and R.Q. Yang, arXiv: 2009.05520; JHEP 03 (2021) 263
RGC, C. Ge, L.Li and R.Q. Yang, arXiv:2112.04206; JHEP 02 (2022) 139
R.Q. Yang, L. Li and RGC, arXiv: 2104.03012; CQG 39 (2022) 035005
RGC, M. N. Duan, L. Li and F.G. Yang, arXiv:2312.11131, JHEP in press

Outline:

1. Introduction
2. No inner horizon theorem for charged black hole with scalar hairs
 - No inner horizon theorem
 - Singularity
 - Hyperbolic black hole with inner horizon
3. The case for black hole with vector hair
4. Towards classifying the interior dynamics of charged black holes with scalar hair
5. The number of black hole horizons with energy condition
6. Conclusions

1、 Introduction: Black hole is one of predictions of GR

Uniqueness theorem of BH in GR:

The most general stationary black hole in Einstein-Maxwell Theory is Kerr-Newman black hole, which is described by three parameters: M , J and Q

Black hole in sky: Kerr black hole (1963): M , J

Kerr-Newman Black Holes :

$$ds^2 = -\left(1 - \frac{2Mr - Q^2}{\rho^2}\right) dt^2 + \frac{\rho^2}{\Delta} dr^2 + \rho^2 d\theta^2 \\ + \left[(r^2 + a^2) + \frac{(2Mr - Q^2)a^2 \sin^2 \theta}{\rho^2}\right] \sin^2 \theta d\varphi^2 - 2 \frac{(2Mr - Q^2)a \sin^2 \theta}{\rho^2} dt d\varphi$$

where

$$\rho^2 = r^2 + a^2 \cos^2 \theta \quad \Delta = r^2 + a^2 - 2Mr + Q^2$$

Horizons: $\Delta = 0 \quad \longrightarrow \quad r_{\pm} = M \pm \sqrt{M^2 - a^2 - Q^2}$

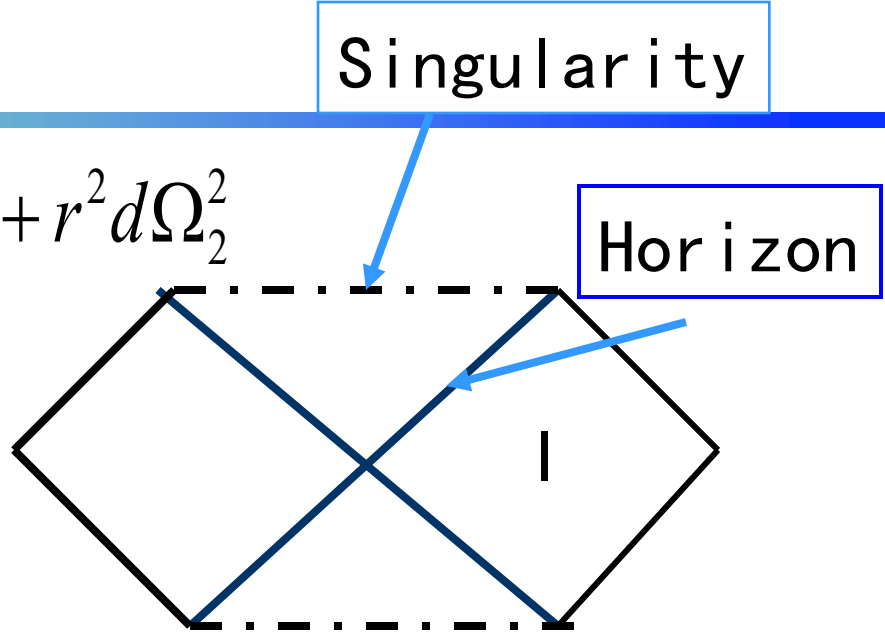
- 1) When $a=0$, Reissner-Nordstrom black hole solution
- 2) When $Q=0$, Kerr black hole solution
- 3) When $a=Q=0$, Schwarzschild black hole solution

Schwarzschild black hole:

$$ds^2 = -\left(1 - \frac{2GM}{r}\right)dt^2 + \left(1 - \frac{2GM}{r}\right)^{-1}dr^2 + r^2d\Omega_2^2$$

Black hole horizon

$$r_+ = 2GM$$



Minimal black hole ?

$$r_+ \gg \lambda_c = 1/M \quad \longrightarrow \quad M \gg 1/\sqrt{G} = M_P$$

Singularities ? $R = R_{\mu\nu} = 0$ $R_{\mu\nu\tau\sigma}R^{\mu\nu\tau\sigma} = \frac{12r_+^2}{r^6}$

spacelike singularity!

Reissner-Nordstrom Black Hole:

$$-\frac{1}{4} F_{\mu\nu} F^{\mu\nu}$$

gravity coupled to a U(1) gauge field

$$ds^2 = -f(r)dt^2 + f^{-1}(r)dr^2 + r^2 d\Omega_2^2$$

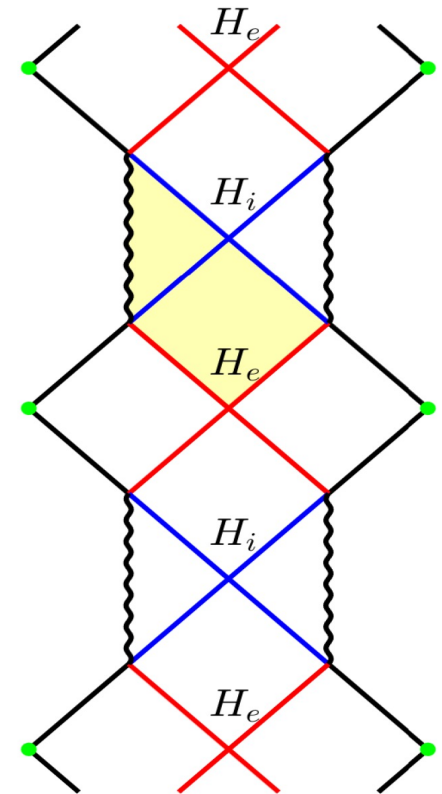
where

$$f(r) = 1 - \frac{2M}{r} + \frac{Q^2}{r^2}$$

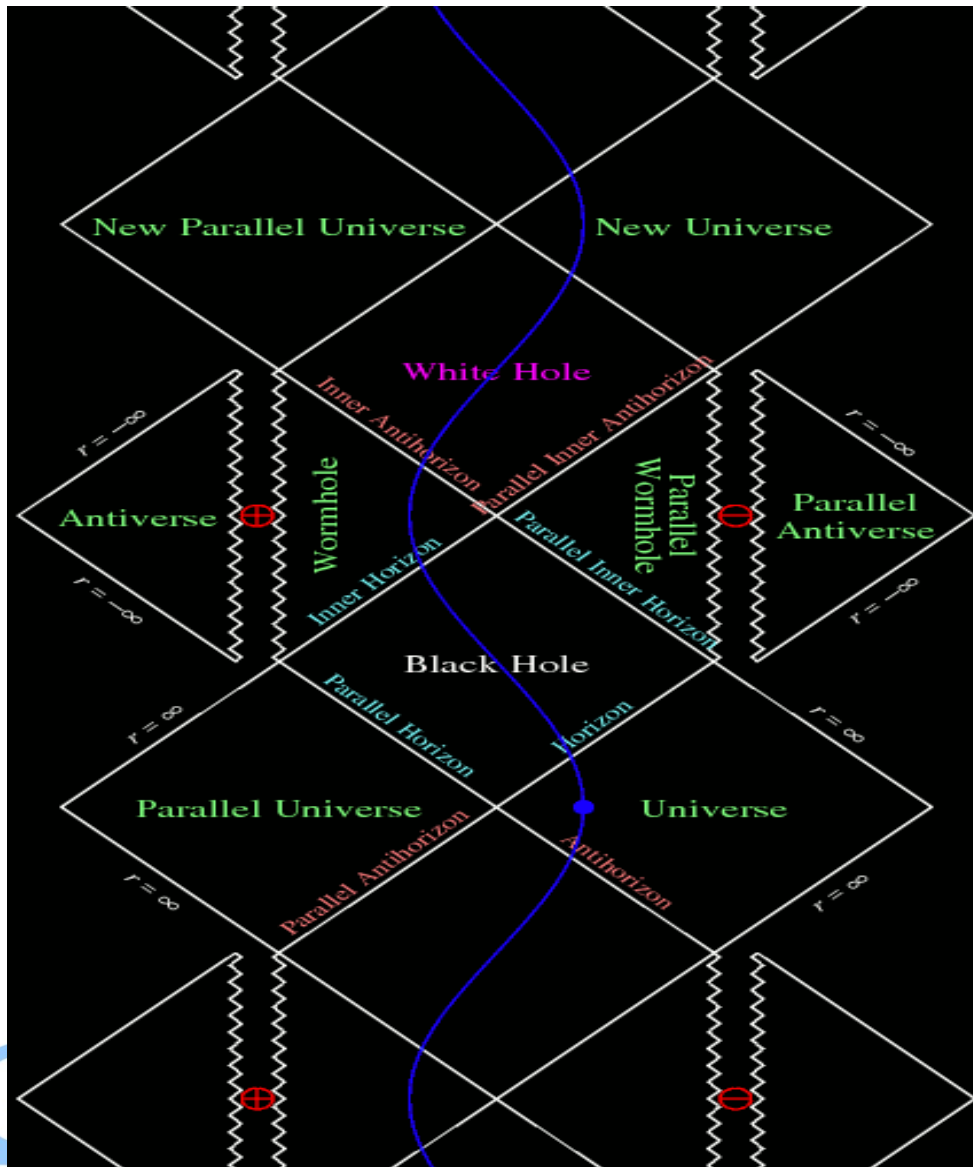
$$F_{tr} = \frac{Q}{r^2}$$

horizons: $r_{\pm} = M \pm \sqrt{M^2 - Q^2}$

The singularity at $r=0$ is timelike!



Penrose diagram of Kerr black hole



$$r_{\pm} = M \pm \sqrt{M^2 - a^2}$$

There is a singularity ring at $r=0$.

Some questions arise naturally:

- 1) The observed black holes are the ones predicted by GR?
- 2) The singularity inside black holes is a generic feature?
if yes, spacelike, nulllike, or timelike?
- 3) Cauchy horizon is stable or unstable? its fate?
 - mass inflation, A. Ori (1991)
 - back reaction of quantum fields

This talk will focus on the internal structure of black holes with various hairs.

2. No inner horizon theorem for charged black hole with scalar

The model: we consider a $(d+2)$ -dimensional gravity theory coupled with a Maxwell field and a charged scalar field:

$$S = \frac{1}{2\kappa_N^2} \int d^{d+2}x \sqrt{-g} [\mathcal{R} + \mathcal{L}_M] ,$$
$$\mathcal{L}_M = -\frac{Z(|\Psi|^2)}{4} F_{\mu\nu} F^{\mu\nu} - (D_\mu \Psi)^* D^\mu \Psi - V(|\Psi|^2)$$

The black hole solution ansatz:

$$ds^2 = \frac{1}{z^2} \left[-f(z) e^{-\chi(z)} dt^2 + \frac{dz^2}{f(z)} + d\Sigma_{d,k}^2 \right] ,$$
$$\Psi = \psi(z) \quad A = A_t(z) dt ,$$

$$d\Sigma_{d,k}^2 = \begin{cases} d\theta^2 + \sin^2 \theta d\Omega_{d-1}^2, & k = 1, \\ \sum_{i=1}^d dx_i^2, & k = 0, \\ d\theta^2 + \sinh^2 \theta d\Omega_{d-1}^2, & k = -1, \end{cases}$$

The equations of motion:

$$V_{\text{eff}}(x) = V(x) - \frac{1}{2} Z(x) z^4 e^{\chi} A_t'^2$$

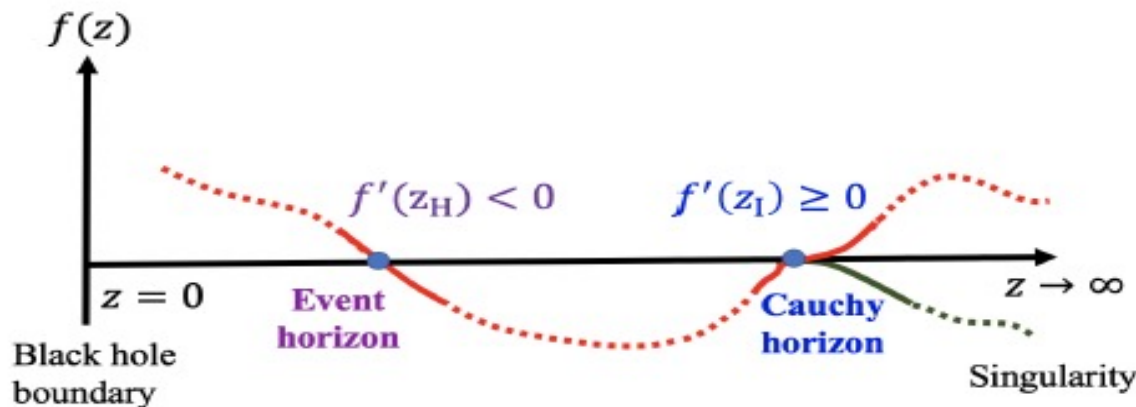
$$z^{d+2} e^{\chi/2} (e^{-\chi/2} z^{-d} f \psi')' = \left[\dot{V}_{\text{eff}}(\psi^2) - \frac{q^2 z^2 e^{\chi} A_t'^2}{f} \right] \psi$$

$$z^d [Z(\psi^2) e^{\chi/2} z^{2-d} A_t']' = \frac{2q^2 \psi^2 e^{\chi/2}}{f} A_t,$$

$$\frac{d}{2} \chi' = z \psi'^2 + \frac{z e^{\chi} q^2 \psi^2 A_t'^2}{f^2},$$

$$\frac{d}{2} \frac{f'}{f} - \frac{z}{2} \psi'^2 - \frac{d(d+1)}{2z} = \frac{V_{\text{eff}}(\psi^2)}{2zf} - \frac{kd(d-1)z}{2f} + \frac{z e^{\chi} q^2 A_t'^2}{2f^2} \psi^2 + \frac{Z(\psi^2) z^3 e^{\chi} A_t'^2}{2f},$$

$$A_t(z_H) = A_t(z_I) = 0$$



$$f'(z_H) < 0, \quad f'(z_I) \geq 0.$$

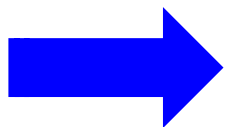
The key observation: the existence of the conserved quantity

$$Q(z) = z^{2-d} e^{\chi/2} [z^{-2} (f e^{-\chi})' - Z A_t A_t'] \\ + 2k(d-1) \int^z y^{-d} e^{-\chi(y)/2} dy.$$

Namely, $Q'(z) = 0$.

Let us evaluate this quantity both at two horizons

$$Q(z_j) = \frac{f'(z_j)}{z_j^d} e^{-\chi(z_j)/2} + 2k(d-1) \int^{z_j} y^{-d} e^{-\chi(y)/2} dy.$$



$$\frac{f'(z_H)}{z_H^d} e^{-\chi(z_H)/2} - \frac{f'(z_I)}{z_I^d} e^{-\chi(z_I)/2} \\ = 2k(d-1) \int_{z_H}^{z_I} y^{-d} e^{-\chi(y)/2} dy$$

$$\frac{f'(z_H)}{z_H^d} e^{-\chi(z_H)/2} - \frac{f'(z_I)}{z_I^d} e^{-\chi(z_I)/2}$$

$$= 2k(d-1) \int_{z_H}^{z_I} y^{-d} e^{-\chi(y)/2} dy.$$

- (1) When $k=0$ or $k=1$: the lhs <0 , while the rhs ≥ 0 ;
- (2) When $k=-1$, the both sides have the same sign:
 counter partner exists, see later. But there only exists
 at most one inner horizon with non zero surface gravity.

The proof is as follows:

- (i) The horizon z_I must be a single root, otherwise we must have $f''(z_I) \leq 0$

$$Q'(z_I) = \frac{f''(z_I)}{z_I^d} e^{-\chi(z_I)/2} - Z z_I^{2-d} e^{\chi(z_I)/2} A_t'(z_I)^2 - 2(d-1)z_I^{-d} e^{-\chi(z_I)/2} < 0.$$

This is not consistent with $Q'(z)=0$! Thus z_i should be a single root with $f''(z_I) > 0$.

- (ii) Suppose there exists a second inner horizon z_{II}

$$\begin{aligned} & \frac{f'(z_I)}{z_I^d} e^{-\chi(z_I)/2} - \frac{f'(z_{II})}{z_{II}^d} e^{-\chi(z_{II})/2} \\ & = -2(d-1) \int_{z_I}^{z_{II}} y^{-d} e^{-\chi(y)/2} dy \end{aligned}$$

$$\begin{aligned} \frac{f'(z_I)}{z_I^d} e^{-\chi(z_I)/2} - \frac{f'(z_{II})}{z_{II}^d} e^{-\chi(z_{II})/2} \\ = -2(d-1) \int_{z_I}^{z_{II}} y^{-d} e^{-\chi(y)/2} dy \end{aligned}$$

The lhs is positive, while the rhs is negative, **therefore the second inner horizon is impossible.**

Singularity

For simplicity, consider $Z=1$ and the kinetic term of the scalar field dominates. In that case, the potential can be neglected.

$$\begin{aligned}\psi &= \sqrt{d}\alpha \ln z + \dots, \quad A'_t = E_s z^{d-2-\alpha^2} + \dots, \\ e^\chi &= \chi_s z^{2\alpha^2} + \dots, \quad f = -f_s z^{1+d+\alpha^2} + \dots,\end{aligned}$$

In that case,

$$Q(z) = \frac{1}{2\kappa_N^2} \int_{\Sigma} Z *F = -\frac{\omega(d)}{2\kappa_N^2} Z z^{2-d} e^{\chi/2} A'_t,$$

The charge approaches to a constant at the singularity,
Namely, the spacelike singularity must be charged.

Introduce the proper time $\tau \sim z^{-(1+d+\alpha^2)/2}$

$$ds^2 = -d\tau^2 + c_t \tau^{2p_t} dt^2 + c_s \tau^{2p_s} d\Sigma_{d,k}^2, \quad (18)$$
$$\psi(z) = -p_\psi \ln \tau,$$

where

$$p_t = \frac{1-d+\alpha^2}{1+d+\alpha^2}, \quad p_s = \frac{2}{1+d+\alpha^2}, \quad p_\psi = \frac{2\sqrt{d}\alpha}{1+d+\alpha^2}. \quad (19)$$

We have

$$p_t + dp_s = 1, \quad p_t^2 + dp_s^2 + p_\psi^2 = 1,$$

The metric has a (generalized) Kasner form!

In the above, the following constraint must be obeyed:

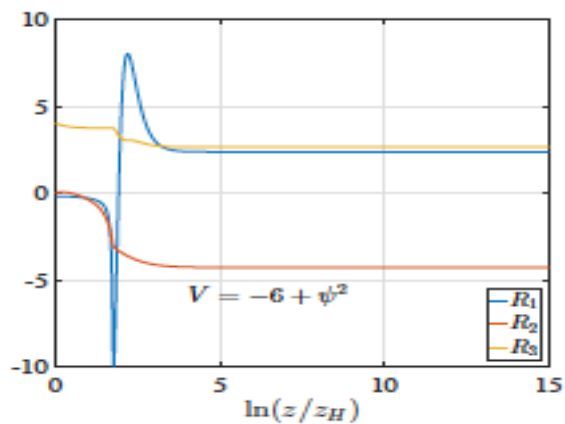
$$\lim_{z \rightarrow \infty} \frac{|V(\psi^2)|}{z^{d+1+\alpha^2}} \ll 1,$$

which allows the potential V to be arbitrary algebraic function, including polynomial function, for example, $V = m^2 \psi^2$.

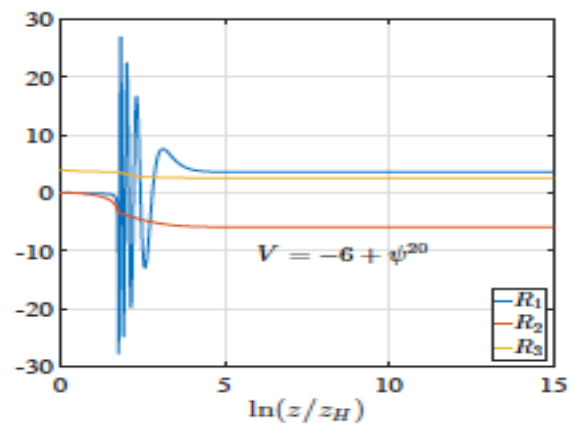
Some examples: we define

$$R_1 = z\psi', \quad R_2 = \ln \left(\frac{z^2 H}{z^2} - h \right), \quad R_3 = 4z^{2-d} e^{\chi/2} A'_t, \quad \text{with } h = e^{-\chi/2} f / z^{1+d}.$$

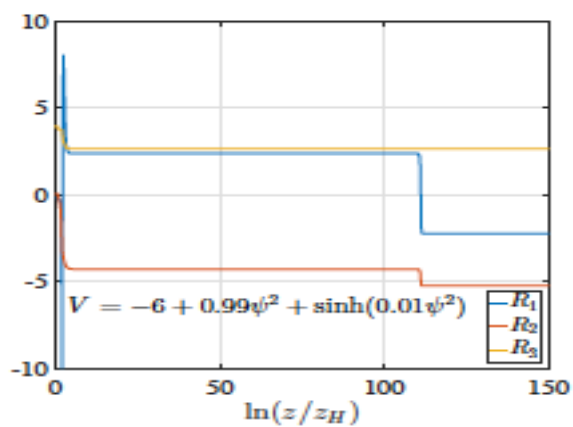
Note that for Kasner geometry, they are constants when $z \rightarrow \infty$



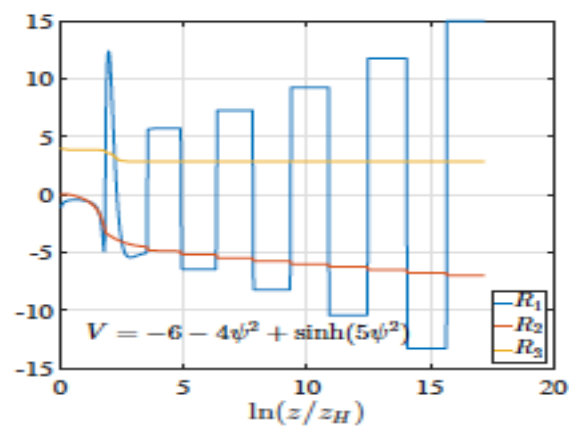
(a)



(b)



(c)



(d)

Hyperbolic black hole with inner horizon

Consider a model in four dimensions:

$$V(\psi^2) = -6 + m^2\psi^2, \quad Z = 1,$$

The equations of motion:

$$\chi' = \frac{2}{d} \left[\frac{\psi^2 A_t^2 q^2}{h^2 z^{2d+1}} + z\psi'^2 \right],$$

$$h' = -\frac{(d-1)k}{z^d} e^{-\chi/2} + \frac{e^{-\chi/2}}{d} \left(\frac{\tilde{Q}^2 z^{d-2}}{2} + \frac{V(\psi^2)}{z^{d+2}} \right),$$

$$\tilde{Q}' = \frac{2\psi^2 A_t q^2}{z^{2d+1} h}, \quad A_t' = \tilde{Q} e^{-\chi/2} z^{d-2},$$

$$\psi'' = -\left(\frac{h'}{h} + \frac{1}{z} \right) \psi' + \left(\frac{\dot{V}(\psi^2) e^{-\chi/2}}{z^{d+3} h} - \frac{A_t^2 q^2}{h^2 z^{2d+2}} \right) \psi,$$

Take the parameter and initial conditions:

$m^2 = -0.18388$ and $q = 1.5$. At the event horizon $z_H = 1.193936$,

$\psi(z_H) \approx 1.10683410$, $\psi'(z_H) \approx 0.115816263$, $\tilde{Q}(z_H) \approx 0.650999915$, $\chi(z_H) = h(z_H) = A_t(z_H) = 0$.

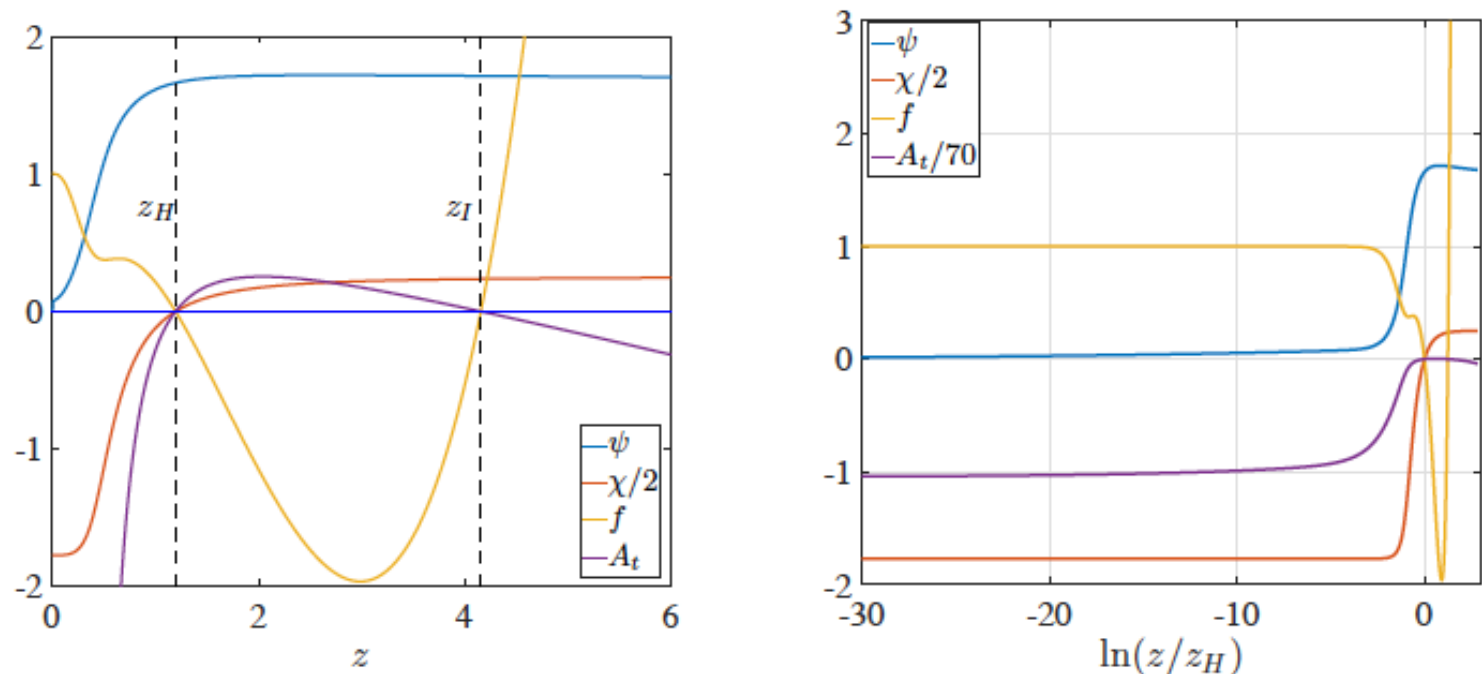


FIG. 3. Numerical solution for hyperbolic case ($k = -1$) with the boundary conditions (30). The hairy black hole has the event horizon at $z_H = 1.193936$. There is a Cauchy horizon at $z_I \approx 4.15699837$ and all functions are smooth at two horizons. From the right panel, we see that $f(0) = 1$, $\psi(0) = 0$, $\chi(0)$ and $A_t(0)$ are both finite, which implies that this solution is indeed an asymptotically AdS black hole. We have considered the four dimensional model with $V(\psi^2) = -6 - 0.18388\psi^2$, $Z = 1$ and $q = 1.5$.

Further discussions:

- No scalar-haired Cauchy horizon theorem in Einstein- Maxwell-Horndeski theories by D. Devecioglu and Mu-In Park (arXiv: 2101.10116)
- No Cauchy horizon theorem for nonlinear electrodynamics black holes with charged scalar hairs by Y. S. An et al, arXiv: 2106.01069 **【 for the hyperbolic horizon case, the Cauchy horizon is ruled out by NED.**
- Black hole singularity across phase transitions by Y. Liu et al, 2108.04554
- Inside an asymptotically flat hairy black hole by O. Dias et al, 2110.06225
- Kasner geometries inside holographic superconductors by L. Sword and D. Vegh, 2112.14177
- The final kasner regime inside black holes with scalar or vector hairs by M. Henneaux, 2202.04155
- Interior of helical black holes by Y. Liu and H. Lyu, 2205.14803
- AdS black holes with a bouncing interior by S. Hartnoll, 2209.12999
- Insights and guidelines on the Cauchy horizon theorem by X.Y. Chew et al, 2308.09225
- Internal structure of hairy rotating black holes in three dimensions, L. L. Gao et al, 2310.15781.....
- ◆ **Vector hair, tensor hair?**
- ◆ **Gravity theories with high curvature terms (e.g., GB theory)?....**

3、 Inside anisotropic black holes with vector hairs

The model we are considering:

$$S = \frac{1}{2\kappa_N^2} \int d^{d+2}x \sqrt{-g} (\mathcal{R} - 2\Lambda + \mathcal{L}_m),$$
$$\mathcal{L}_m = -\frac{1}{4} F_{\mu\nu} F^{\mu\nu} - \frac{1}{2} \rho_{\mu\nu}^\dagger \rho^{\mu\nu} - m^2 \rho_\mu^\dagger \rho^\mu + iq\gamma \rho_\mu \rho_\nu^\dagger F^{\mu\nu},$$

where $F_{\mu\nu} = \nabla_\mu A_\nu - \nabla_\nu A_\mu$ and $\rho_{\mu\nu} = D_\mu \rho_\nu - D_\nu \rho_\mu$ with $D_\mu = \nabla_\mu - iqA_\mu$.

(R. G. Cai et al, arXiv:1309.4877, a holographic p-wave model)

The ansatz for metric and matter field:

$$ds^2 = e^{2\alpha(r)} [-h(r)dt^2 + e^{2\eta(r)} dx^2 + d\vec{y}_{d-1}^2] + e^{2\beta(r)} \frac{dr^2}{h(r)},$$
$$\rho_\nu dx^\nu = \rho_x(r) dx, \quad A_\nu dx^\nu = A_t(r) dt,$$

I Here $\beta(r)$ can be set to zero as a gauge choice.

The effective action:

$$S = \frac{V_{d+1}}{2\kappa_N^2} \int dr \mathcal{L}_{\text{eff}}(\alpha, \alpha', \alpha''; \eta, \eta', \eta''; h, h', h''; \beta, \beta'; A_t, A'_t; \rho_x, \rho'_x),$$

The key observation: **there is a scaling symmetry**

$$\begin{aligned} \alpha(r) &\rightarrow \alpha(r) - \log(\lambda), & \beta(r) &\rightarrow \beta(r) + (d+1)\log(\lambda), & h(r) &\rightarrow \lambda^{2(d+1)}h(r), \\ A_t(r) &\rightarrow \lambda^d A_t(r), & \rho_x(r) &\rightarrow \lambda^{-1}\rho_x(r), & \eta(r) &\rightarrow \eta(r), \end{aligned}$$

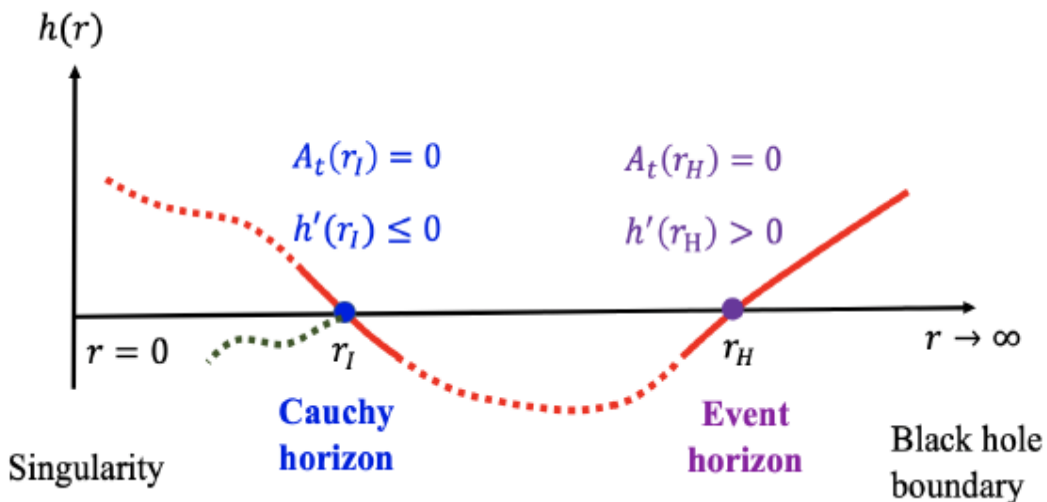
There is an associated conserved charge:

$$\begin{aligned} Q &= \sum_{a=\{\alpha, \eta, h, \beta, A_t, \rho_x\}} -F_a \left(\frac{\partial \mathcal{L}_{\text{eff}}}{\partial \mathcal{F}'_a} \right) - \frac{dF_a}{dr} \left(\frac{\partial \mathcal{L}_{\text{eff}}}{\partial \mathcal{F}''_a} \right) + F_a \frac{d}{dr} \left(\frac{\partial \mathcal{L}_{\text{eff}}}{\partial \mathcal{F}''_a} \right), \\ &= de^{(d-1)\alpha+\eta} (e^{2\alpha} h' - A_t A'_t) - 2he^{(d-1)\alpha-\eta} (e^{2(\alpha+\eta)} \eta' + \rho_x \rho'_x), \end{aligned}$$

No Cauchy horizon:

$$h(r_H) = h(r_I) = 0, \quad r_I < r_H.$$

$$A_t(r_H) = A_t(r_I) = 0,$$



$$e^{(d+1)\alpha(r_H)+\eta(r_H)} h'(r_H) = e^{(d+1)\alpha(r_I)+\eta(r_I)} h'(r_I).$$

$$h'(r_H) > 0, \quad h'(r_I) \leq 0.$$



No solution



No inner horizon

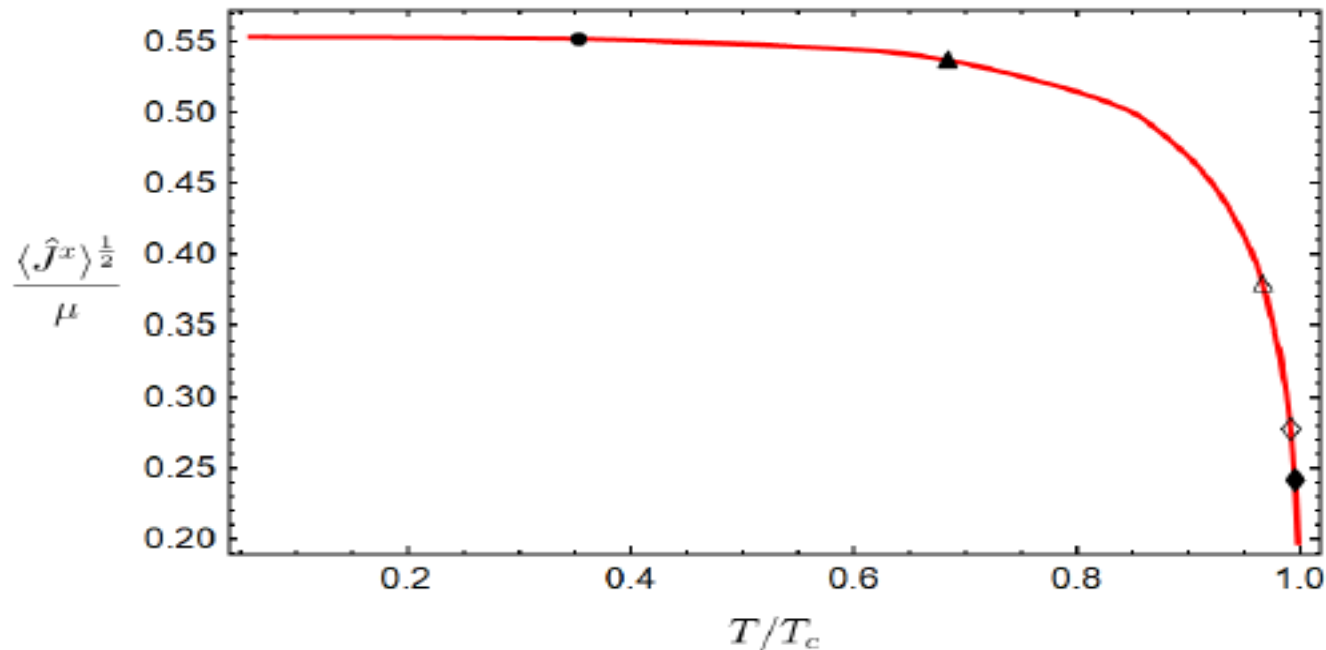
Anisotropic black hole: p-wave superconductor

$$ds^2 = \frac{1}{z^2} \left[-f(z) e^{-\chi(z)} dt^2 + \frac{dz^2}{f(z)} + u(z) dx^2 + d\vec{y}_{d-1}^2 \right].$$

$$\rho_\nu dx^\nu = \rho_x(z) dx, \quad A_\nu dx^\nu = A_t(z) dt,$$

Near $z=0$:

$$A_t = \mu + \dots, \quad \rho_x = \rho_{x+} z^{\Delta-1} + \dots, \quad \Delta = \frac{d+1 + \sqrt{(d-1)^2 + 4m^2}}{2},$$



Dynamical epochs inside: Anisotropic Kasner cosmology

$$ds^2 = \frac{1}{z^2} \left[-f(z) e^{-\chi(z)} dt^2 + \frac{dz^2}{f(z)} + u(z) dx^2 + d\vec{y}_{d-1}^2 \right].$$

$$\rho_\nu dx^\nu = \rho_x(z) dx, \quad A_\nu dx^\nu = A_t(z) dt,$$

In this coordinate, the AdS boundary is at $z=0$, while the singularity is assumed at $z=\infty$. Near the singularity, one has (neglecting the contribution of matter fields)

$$u \sim z^{n_u}, \quad f \sim z^{n_f}, \quad \chi \sim n_\chi \ln z + \chi_0, \quad \rho_x \sim z^{n_\rho} + \rho_0, \quad A_t \sim z^{n_A} + A_0,$$

The solution:

$$n_\rho = n_u - 2, \quad n_A = d - 1 - \frac{(d-1)n_u}{2d - n_u},$$
$$n_f = -n_u + \frac{2d(d+1) - 2n_u}{2d - n_u}, \quad n_\chi = -n_u + \frac{(2d-2)n_u}{2d - n_u}.$$

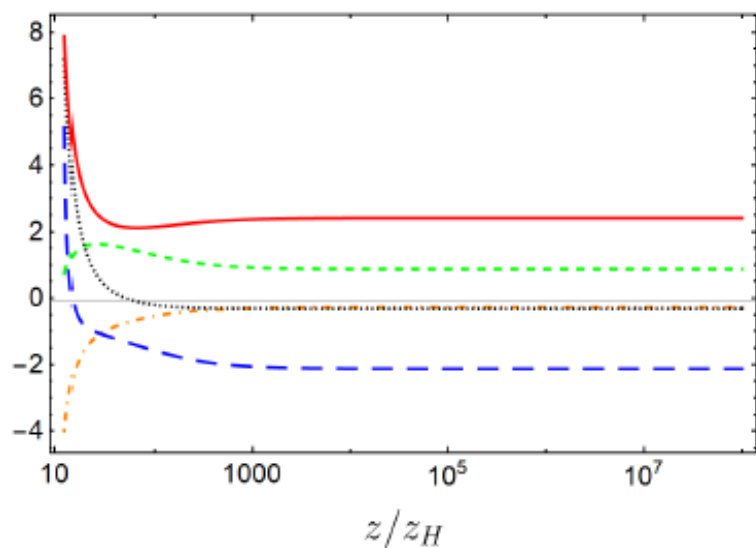
Changing the z coordinate to the proper time τ via $\tau \sim z^{-n_f/2}$, we obtain

$$ds^2 = -d\tau^2 + c_t \tau^{2p_t} dt^2 + c_x \tau^{2p_x} dx^2 + \sum_{i=1}^{d-1} c_{y_i} \tau^{2p_{y_i}} dy_i^2.$$

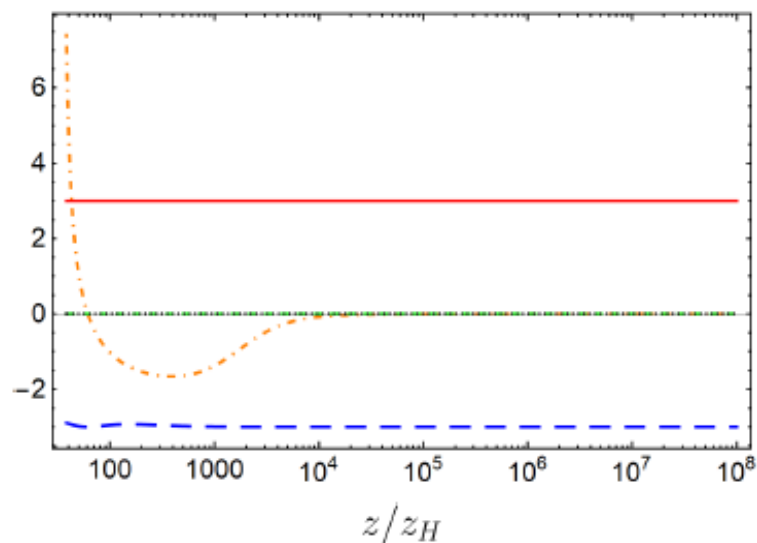
$$p_t = \frac{n_\chi - n_f + 2}{n_f}, \quad p_x = \frac{2 - n_u}{n_f}, \quad p_{y_i} = \frac{2}{n_f}.$$

$$p_t + p_x + \sum_{i=1}^{d-1} p_{y_i} = 1, \quad p_t^2 + p_x^2 + \sum_{i=1}^{d-1} p_{y_i}^2 = 1,$$

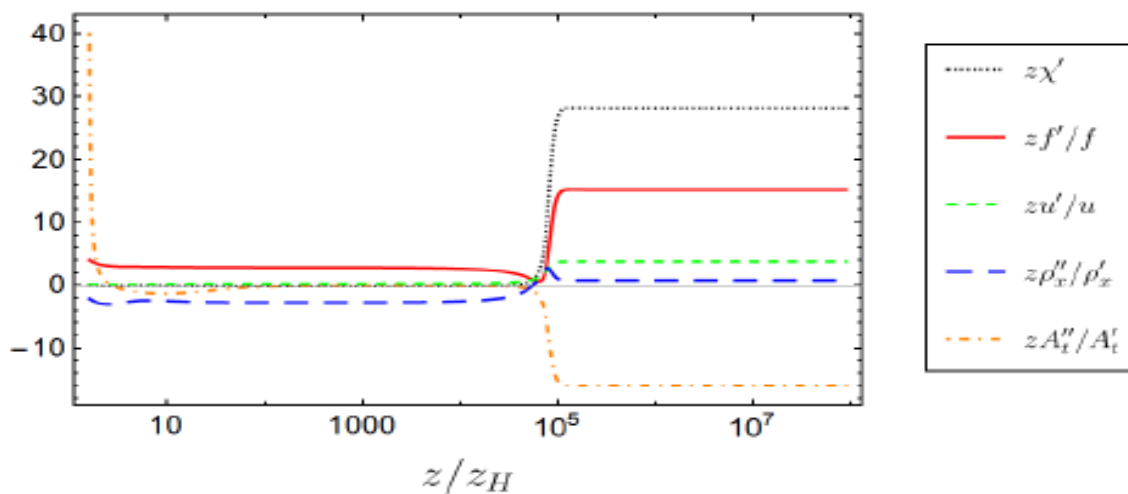
Numeric examples with $d = 2, m = 0, q = 3/2$.



(a) $T_{\blacklozenge}/T_c = 0.995$



(b) $T_{\bullet}/T_c = 0.168$



(c) $T_{\blacktriangle}/T_c = 0.684$

Analytic and numeric comparison:

		Numerical Values	Analytic Values	Relative Errors
$T_{\blacklozenge}/T_c = 0.995$ $n_u = 1.1227740945654$	n_f	2.2674538998442	2.2674538998526	3.7×10^{-12}
	n_χ	-0.3423181057185	-0.3423181057293	3.1×10^{-11}
	n_ρ	-0.8772259054207	-0.8772259054345	1.6×10^{-11}
	n_A	0.6097720055765	0.6097720055819	8.8×10^{-12}
$T_{\blacktriangle}/T_c = 0.684$ $n_u = 3.76376613$	n_f	15.16872553	15.16860713	7.8×10^{-6}
	n_χ	28.10121840	28.10098041	8.5×10^{-6}
	n_ρ	1.76377015	1.76376613	2.3×10^{-6}
	n_A	-14.93249248	-14.93237327	8.0×10^{-6}
$T_{\bullet}/T_c = 0.168$ $n_u = 6.57 \times 10^{-13}$	n_f	2.999999999998551	2.999999999999507	3.2×10^{-13}
	n_χ	$-3.28521349 \times 10^{-13}$	$-3.28529790 \times 10^{-13}$	0.000026
	n_ρ	-1.99998716	-1.99999999	6.4×10^{-6}
	n_A	0.999997794	0.99999999	2.2×10^{-6}

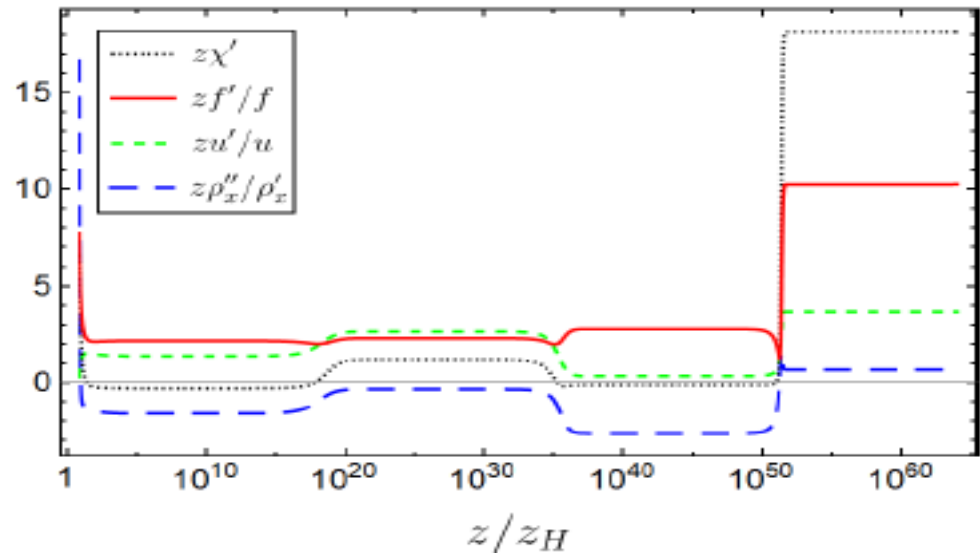
Kanser alternation and flipping of powers

We find that the interior geometry near singularity does not experience only one Kasner epoch, but several ones as $z \rightarrow \infty$, and one has:

$$d = 2, m = 0, q = 3/2 \text{ and } T/T_c = 0.983.$$

For $n_u < 2$, $n_u + \tilde{n}_u = 4$,

For $2 < n_u < 4$, $n_A = -\tilde{n}_A$.



Numerical values:

Kasner epochs (z/z_H)	$10^5 \sim 10^{18}$	$10^{18} \sim 10^{34}$	$10^{34} \sim 10^{51}$	$10^{51} \sim 10^{64}$
n_A	0.474604	-0.908835	0.908599	-9.903578
n_u	1.375555	2.624619	0.336036	3.663967
Sum	4.000168		4.000002	

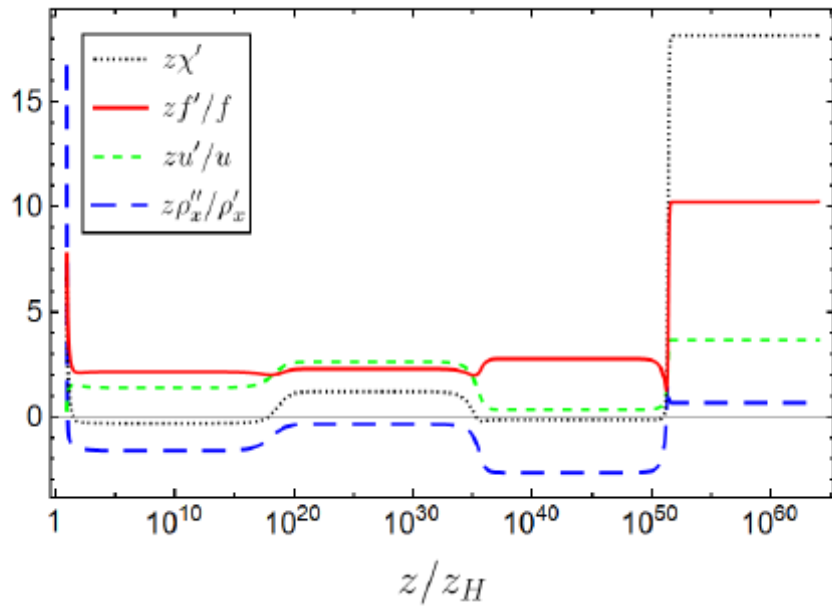
Five more examples:

$$n_u + \tilde{n}_u = 4, \quad n_A = -\tilde{n}_A.$$

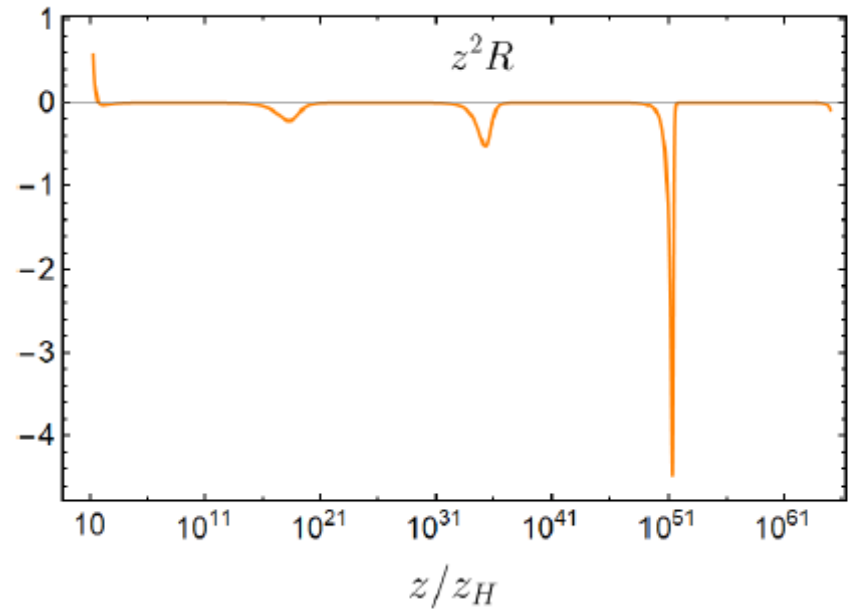
	Kasner epochs (z/z_H)	n_u	n_A	Sum
$T/T_c = 0.998$	$10^3 \sim 10^{146}$	1.173335	0.584905	4.000000
	$10^{146} \sim 10^{290}$	2.826665	-1.409087	
	$10^{290} \sim 10^{436}$	-2.769187	1.409087	
$T/T_c = 0.997$	$10^2 \sim 10^{127}$	1.240325	0.550554	4.000000
	$10^{127} \sim 10^{250}$	2.759675	-1.224960	
	$10^{250} \sim 10^{380}$	-1.160680	1.224893	
$T/T_c = 0.994$	$10^3 \sim 10^{48}$	1.218098	0.562135	4.000000
	$10^{48} \sim 10^{95}$	2.781902	-1.283808	
	$10^{95} \sim 10^{140}$	-1.585010	1.283793	
$T/T_c = 0.991$	$10^3 \sim 10^{32}$	1.122742	0.609818	3.999968
	$10^{32} \sim 10^{64}$	2.877226	-1.562605	
	$10^{64} \sim 10^{90}$	-5.145021	1.562602	
$T/T_c = 0.985$	$10^2 \sim 10^{16}$	1.014178	0.660504	4.000206
	$10^{16} \sim 10^{32}$	2.986028	-1.944810	
	$10^{32} \sim 10^{45}$	-68.574549	1.944884	

Table 4: The values n_u and n_A at three Kasner epochs for five different temperatures. The sum of n_u of the first and second Kasner epochs are, within numerical error, equal to 4 (blue), while the values of n_A at the second and third Kasner epochs are opposite values (red). Here $d = 2$, $m^2 = 0$ and $q = 3/2$.

Never-ending Kasner alternations:



(a)

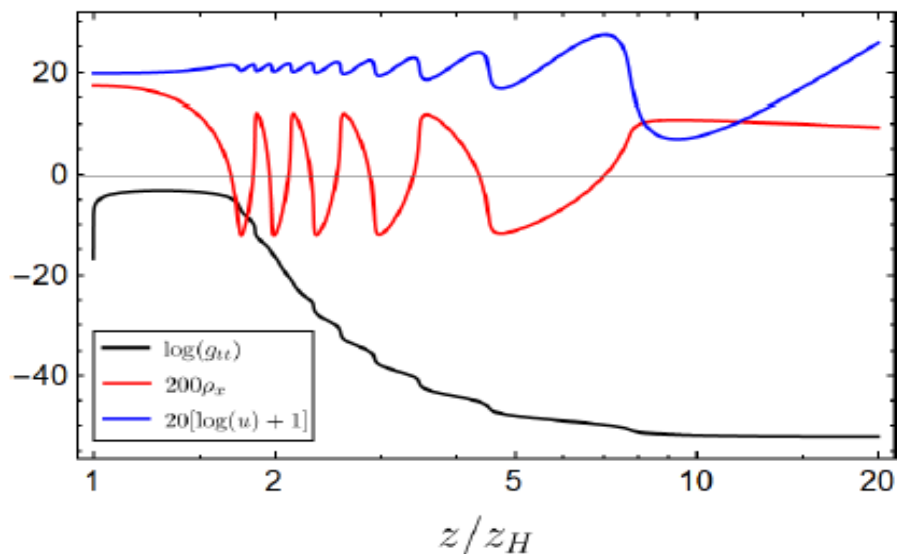


(b)

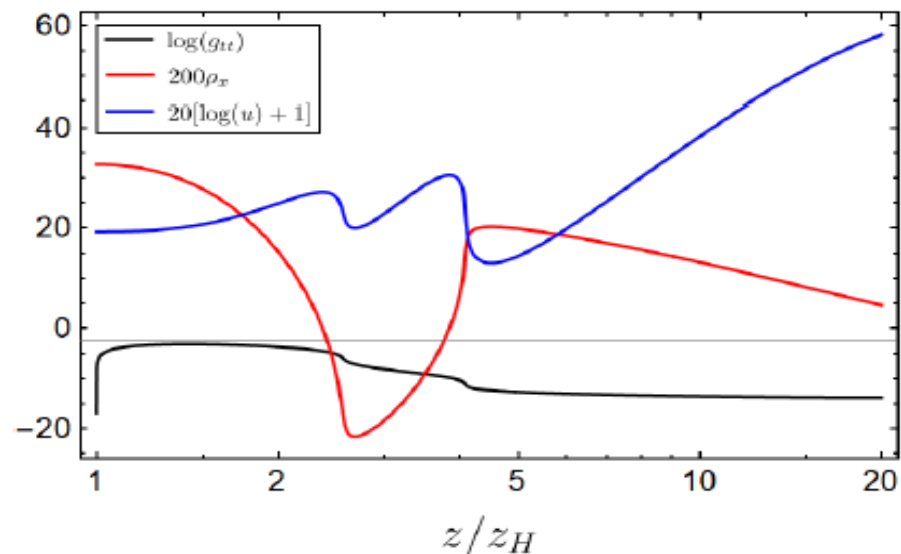
Figure 4: Kasner epochs at $T/T_c = 0.983$. Four Kasner epochs in the interior are shown in (a). The contribution from the right terms of the last equation of (8), denoted as R , is plotted in (b). While R is negligible in each Kasner region, it does become important in the transition region between adjacent Kasner epochs. Here $d = 2$, $m^2 = 0$ and $q = 3/2$.

Collapse of ER bridge and Josephson oscillations:

When T is above T_c , the solution is the RN-AdS black hole, when T is slightly less than T_c , the Cauchy horizon will disappear. The geometry near the would-be inner horizon:



(a) $T_\Delta/T_c = 0.991$



(b) $T_\Delta/T_c = 0.966$

The anisotropic factor $u(z)$ also oscillates with a half period of the vector condensate. When T decreases, the non-linear dynamics become less dramatic.

Further considerations: No Cauchy horizon

(1) The case one:

$$\mathcal{L}_m^{\text{ext}} = -\frac{Z(\rho_\mu^\dagger \rho^\mu, |\rho_\mu \rho^\mu|^2)}{4} F_{\mu\nu} F^{\mu\nu} - \frac{1}{2} \rho_{\mu\nu}^\dagger \rho^{\mu\nu} - V(\rho_\mu^\dagger \rho^\mu, |\rho_\mu \rho^\mu|^2) + iq\gamma \rho_\mu \rho_\nu^\dagger F^{\mu\nu},$$

$$Q = e^{(d-1)\alpha+\eta}(e^{2\alpha}h' - ZA_t A'_t) - \frac{2h}{d} e^{(d-1)\alpha-\eta}(e^{2(\alpha+\eta)}\eta' + \rho_x \rho'_x),$$

(2) The case two:

$$S_{GB} = \frac{1}{2\kappa_N^2} \int d^{d+2}x \sqrt{-g} \left[\mathcal{R} + \alpha_{GB}(\mathcal{R}^2 - 4\mathcal{R}_{\mu\nu}\mathcal{R}^{\mu\nu} + \mathcal{R}_{\mu\nu\gamma\delta}\mathcal{R}^{\mu\nu\gamma\delta}) - 2\Lambda + \mathcal{L}_m \right]$$

$$Q = de^{(d-1)\alpha+\eta}(e^{2\alpha}h' - A_t A'_t) - 2he^{(d-1)\alpha-\eta}(e^{2(\alpha+\eta)}\eta' + \rho_x \rho'_x) + 2(d-1)(d-2)\alpha_{GB}e^{(d+1)\alpha+\eta}h\alpha' [2h\alpha'\eta' - h'(d\alpha' + 2\eta')],$$

4. Classifying the interior dynamics of black holes with scalar

The setup

$$S = \frac{1}{2\kappa_N^2} \int d^{d+1}x \sqrt{-g} [R + \mathcal{L}] ,$$
$$\mathcal{L} = -\frac{1}{2}(\partial_\mu\psi)^2 - \mathcal{F}(\psi)(\partial_\mu\theta - qA_\mu)^2 - V(\psi) - \frac{Z(\psi)}{4}F_{\mu\nu}F^{\mu\nu}$$

The hairy black hole solution takes the form:

$$ds^2 = \frac{1}{z^2} \left[-f(z)e^{-\chi(z)}dt^2 + \frac{dz^2}{f(z)} + d\Sigma_{d-1,k}^2 \right], \quad \psi = \psi(z), \quad A = A_t(z)dt,$$

Here $d\Sigma_{d-1,k}^2$ denotes the line element of unit sphere ($k=1$), planar ($k=0$) or hyperbolic sphere ($k=-1$) in $d-1$ dim

We take $\theta=0$ without loss generality, then

$$\psi'' = - \left(\frac{1}{z} + \frac{h'}{h} \right) \psi' - \frac{q^2 A_t^2}{z^{2d} h^2} \frac{d\mathcal{F}}{d\psi} + \frac{e^{-\chi/2}}{z^{d+2} h} \frac{dV}{d\psi} + \frac{e^{\chi/2}}{2z^{d-2} h} \frac{dZ}{d\psi},$$

$$\left(\frac{e^{\chi/2} Z A_t'}{z^{d-3}} \right)' = \frac{2q^2 A_t}{z^{2d-1} h} \mathcal{F},$$

$$(d-1)\chi' = z\psi'^2 + \frac{2q^2 A_t^2}{z^{2d-1} h^2} \mathcal{F},$$

$$h' = \frac{e^{-\chi/2}}{d-1} \left(-\frac{k(d-1)(d-2)}{z^{d-1}} + \frac{V}{z^{d+1}} + \frac{e^{\chi}}{2z^{d-3}} Z A_t'^2 \right), \quad h = z^{-d} e^{-\chi/2} f$$

In this coordinate, the boundary is at $z=0$, while the singularity would be at $z \rightarrow \infty$. And the associated thermodynamics

$$T = -\frac{e^{-\chi(z_H)/2} f'(z_H)}{4\pi}, \quad s = \frac{2\pi}{\kappa_N^2 z_H^{d-1}}.$$

ITP Note that one has $A_t(z_H) = 0$ once $q \neq 0$.

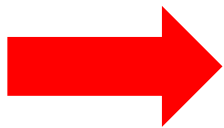
Kasner Epoch:

In this case, the contributions from F and V are negligible. At large z limit

$$\psi'' = -\frac{1}{z}\psi', \quad \left(\frac{e^{\chi/2}A'_t}{z^{d-3}}\right)' = 0, \quad (d-1)\chi' = z\psi'^2,$$
$$h' = \frac{1}{2(d-1)} \left(\frac{e^{\chi/2}A'_t}{z^{d-3}}\right)^2 z^{d-3}e^{-\chi/2},$$

One has the solution:

$$\psi = \alpha \ln z + C_\psi, \quad \chi = \frac{\alpha^2}{d-1} \ln z + C_\chi,$$
$$A'_t = C_{A_t} z^{d-3} e^{-\chi/2}, \quad h' = C_h z^{d-3} e^{-\chi/2},$$



$$ds^2 = \frac{1}{z^2} \left[-\frac{dz^2}{C_f z^d e^{\chi/2}} + C_f z^d e^{-\chi/2} dt^2 + d\Sigma_{d-1,k}^2 \right], \quad \psi \simeq \alpha \ln z,$$

Introducing the proper time: $\tau \sim z^{-\left(\frac{d}{2} + \frac{\alpha^2}{4(d-1)}\right)}$.

$$ds^2 = -d\tau^2 + c_t \tau^{2p_t} dt^2 + c_s \tau^{2p_s} d\Sigma_{d-1,k}^2, \quad \psi \simeq -\sqrt{2} p_\psi \ln \tau,$$

where

$$p_t = \frac{\alpha^2 - 2(d-1)(d-2)}{\alpha^2 + d(d-1)}, \quad p_s = \frac{4(d-1)}{\alpha^2 + d(d-1)}, \quad p_\psi = \frac{2\sqrt{2}(d-1)\alpha}{\alpha^2 + d(d-1)},$$

with c_t and c_s constants. One immediately finds that

$$p_t + (d-1)p_s = 1, \quad p_t^2 + (d-1)p_s^2 + p_\psi^2 = 1,$$

The (generalized)
Kasner geometry

These constants are all determined by alpha, called Kasner exponent. It is easy to check that the solution makes sense if

$$\begin{aligned} \mathcal{O}\left(\frac{q^2 A_t^2}{z^{2d} h^2} \frac{d\mathcal{F}}{d\psi}\right) &< \mathcal{O}\left(\frac{1}{z^{2d-1}}\right), & \mathcal{O}\left(\frac{e^{-\chi/2}}{z^{d+2} h} \frac{dV}{d\psi}\right) &< \mathcal{O}\left(\frac{1}{z^{d+1}}\right), \\ \mathcal{O}\left(\frac{q^2 A_t}{z^{2d-1} h} \mathcal{F}\right) &< \mathcal{O}\left(\frac{1}{z^{2d-2}}\right), & \mathcal{O}\left(\frac{2q^2 A_t^2}{z^{2d-1} h^2} \mathcal{F}\right) &< \mathcal{O}\left(\frac{1}{z^{2d-2}}\right), \\ \mathcal{O}\left(\frac{e^{-\chi/2}}{z^{d-1}}\right) &< \mathcal{O}\left(\frac{1}{z^{d-1}}\right), & \mathcal{O}\left(\frac{V e^{-\chi/2}}{z^{d+1}}\right) &< \mathcal{O}\left(\frac{1}{z^d}\right), \end{aligned}$$

this allows V and F to be arbitrary algebraic functions, including polynomial functions. Namely once these conditions are obeyed, the neglected terms in EOMs will not change the solutions.

Kasner Inversion:

Once the above assumption is invalid, the solution will become unstable. A particularly simple case is triggered by the h'/h term. Interestingly, this alternation caused by the non-integrability of h' will make itself come back to be integrable and will enter a new stable Kasner epoch. This is called Kasner Inversion.

Inside the event horizon, one has $h < 0$, while $h'(z) \sim z^{d-3-\frac{\alpha^2}{2(d-1)}}$.

To have a stable Kasner epoch down to the singularity, the integral of h' should be finite, otherwise the new dynamics will come into play. The breakdown of the integrability of h' :

$$d-3-\frac{\alpha^2}{2(d-1)} > -1 \Rightarrow |\alpha| < \sqrt{2(d-1)(d-2)}.$$

In this case, the background becomes unstable and the term h'/h cannot be dropped. Then the dynamics is determined by the equations

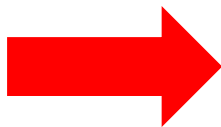
$$\frac{1}{z}(z\psi')' = -\frac{h'}{h}\psi', \quad h' = \frac{1}{2(d-1)} \left(\frac{e^{\chi/2} A_t'}{z^{d-3}} \right)^2 z^{d-3} e^{-\chi/2}.$$

Here h' is determined by the kinetic term of the gauge field.

Take the form: $\psi(z) = \int^z \frac{\tilde{\alpha}(s)}{s} ds.$



$$2z(d-1)\tilde{\alpha}\tilde{\alpha}'' - 4z(d-1)\tilde{\alpha}'^2 + \tilde{\alpha}'\tilde{\alpha}(\tilde{\alpha}^2 - 2(d-1)(d-3)) = 0.$$



$$2(d-2) \ln \left[\frac{z}{z_I} \right] + \frac{2c_1 \sqrt{d-1}}{\sqrt{(d-1)c_1^2 - 2d + 4}} \operatorname{arctanh} \left[\frac{c_1(d-1) - \tilde{\alpha}[z]}{\sqrt{d-1} \sqrt{(d-1)c_1^2 - 2d + 4}} \right] \\ + 2 \ln \left| \frac{\tilde{\alpha}[z]}{c_1(d-1)} \right| + 2 \ln \left| \frac{c_1^2(d-1)^2 - 2(d-1)(d-2)}{\tilde{\alpha}[z]^2 - 2(d-1)c_1\tilde{\alpha}[z] + 2(d-1)(d-2)} \right| = 0,$$

The two exponent alpha for the Kasner epoch before and after the Kasner inversion are the roots:

$$\tilde{\alpha}^2 - 2c_1(d-1)\tilde{\alpha} + 2(d-1)(d-2) = 0.$$

These two roots obey

$$\alpha\alpha_I = 2(d-1)(d-2),$$

Here alpha is the one before the inversion, while alpha_I is the one after the inversion



Suppose there is a Kasner epoch with $|\alpha| < \sqrt{2(d-1)(d-2)}$
There will be a new Kasner epoch with

$$|\alpha_I| = 2(d-1)(d-2)/|\alpha| > \sqrt{2(d-1)(d-2)}.$$

Kasner Transition:

When one considers the coupling function F with an exponential form

$$\mathcal{F}(\psi) \sim e^{\kappa\psi}$$

The background solution will be destroyed and a new Kasner transformation process will appear.

One can see when

$$\mathcal{O}\left(\frac{A_t^2}{z^{2d}h^2} \frac{d\mathcal{F}}{d\psi}\right) = \mathcal{O}\left(\frac{z^{\kappa\alpha}}{z^{2d}}\right) \geq \mathcal{O}\left(\frac{\psi'}{z}\right) \longrightarrow \kappa\alpha > (2d-2),$$

The term with $dF/d\psi$ cannot be dropped. In this case, one has

$$\frac{1}{z}(z\psi')' \simeq \frac{e^{\kappa\psi}}{z^{2d}}.$$

$$z\tilde{\alpha}'' + (2d-1)\tilde{\alpha}' - \kappa\tilde{\alpha}\tilde{\alpha}' = 0. \quad \tilde{\alpha}(z) = \frac{2d-2 - c_1 \tanh[c_1 \ln(z/z_T)]}{\kappa},$$

One has the transformation law for the Kasner transition

$$\alpha + \alpha_T = \frac{2}{\kappa}(2d-2).$$



Suppose there is a Kasner epoch with $\kappa\alpha > (2d-2)$
This transformation law shows that the Kasner transition process will decrease the amplitude of alpha until the condition is destroyed.

In addition, the transformation not only depends on the dimension, but also the parameter kappa.

Classification of Kasner Alternation:

As we have seen that the Kasner transition causes alpha to decrease while the Kasner inversion makes alpha increase. When these two processes are triggered alternately, it could lead to an infinite chaotic oscillation of Kasner epochs.

Case I: $\sqrt{2(d-1)(d-2)} < 2(d-1)/|\kappa|$ (left panel of Fig. 1).

The Kasner transition occurs when $|\alpha| > 2(d-1)/|\kappa|$ and the Kasner inversion occurs when $|\alpha| < \sqrt{2(d-1)(d-2)}$. Once $\sqrt{2(d-1)(d-2)} < |\alpha| < 2(d-1)/|\kappa|$, both the Kasner transformations will not be triggered, thus the system settles down to a stable Kasner epoch.

Case II: $\sqrt{2(d-1)(d-2)} = 2(d-1)/|\kappa|$ (middle panel of Fig. 1).

In this critical case, $|\alpha| = \sqrt{2(d-1)(d-2)} = 2(d-1)/|\kappa|$ is the only fixed point. Therefore, for the initial value of $\alpha \neq \sqrt{2(d-1)(d-2)} = 2(d-1)/|\kappa|$, there will be an infinite Kasner alternations towards the singularity.

Case III: $\sqrt{2(d-1)(d-2)} > 2(d-1)/|\kappa|$ (right panel of Fig. 1).

When $|\alpha| > \sqrt{2(d-1)(d-2)}$, the Kasner transition develops, and when $|\alpha| < 2(d-1)/|\kappa|$, the Kasner inversion appears.

Nevertheless, for $2(d-1)/|\kappa| < |\alpha| < \sqrt{2(d-1)(d-2)}$ (the overlapping region in the right panel of Fig. 1), both the contributions from h'/h and \mathcal{F} to (2.3) play important roles. The complex competition between the Kasner inversion and the transition could occur. So far, we have not been able to give an analytical description of this overlapping regime.

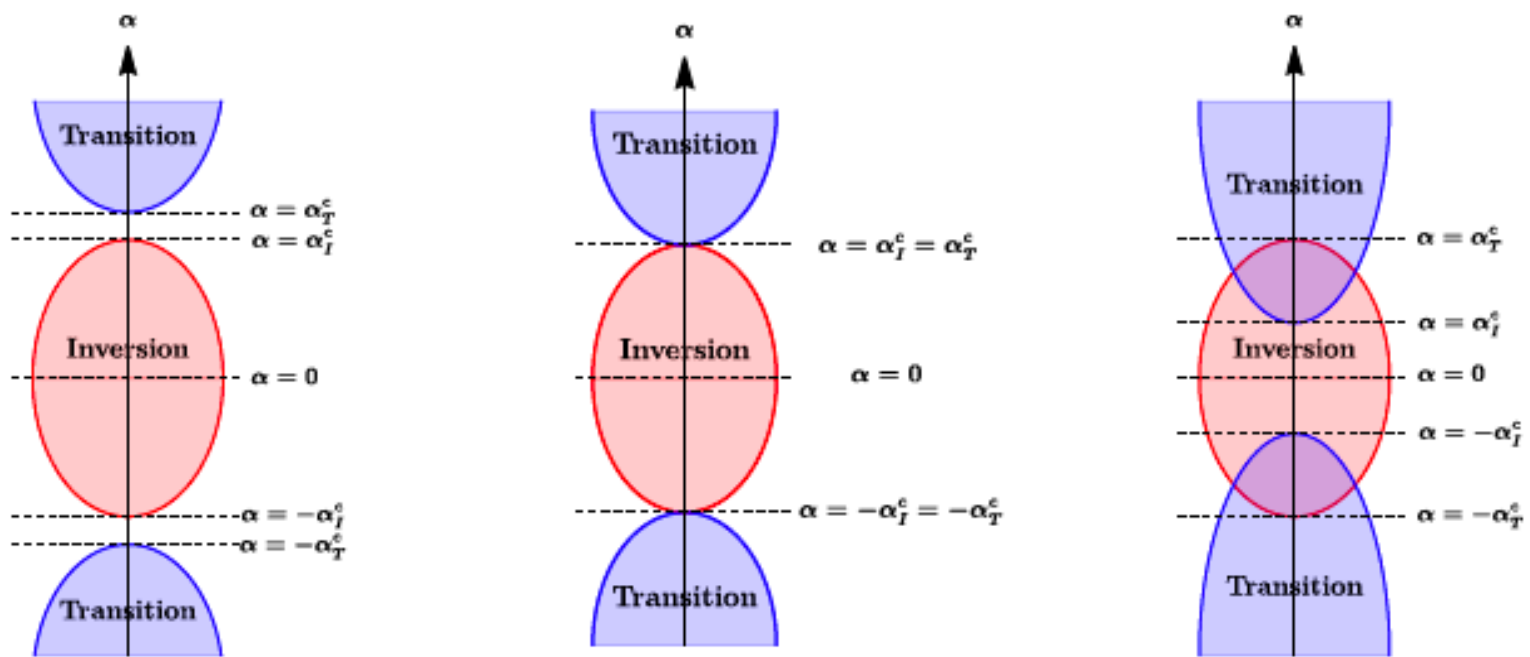


Figure 1: Classification for the possible alternation of Kasner epochs for a theory with an exponential coupling $\mathcal{F}(\psi) \sim e^{\kappa\psi}$. Give a Kasner epoch with the exponent $\alpha = z\psi'$ and denote $\alpha_{\mathcal{I}}^c = \sqrt{2(d-1)(d-2)}$ and $\alpha_{\mathcal{T}}^c = 2(d-1)/|\kappa|$. A Kasner transition triggers when α falls into the blue region ($|\alpha| > \alpha_{\mathcal{T}}^c$), and a Kasner inversion appears when α is in the red region ($|\alpha| < \alpha_{\mathcal{I}}^c$). The Kasner alternation can be divided into three classes depending on the spatial dimension d and the coupling constant κ . **Left panel:** $\alpha_{\mathcal{I}}^c < \alpha_{\mathcal{T}}^c$. There exist a stable region with $\alpha_{\mathcal{I}}^c < |\alpha| < \alpha_{\mathcal{T}}^c$. **Middle panel:** $\alpha_{\mathcal{I}}^c = \alpha_{\mathcal{T}}^c = \sqrt{2(d-1)(d-2)}$. There will be an infinite sequence of Kasner alternations towards the singularity, except for the fine-tuning with $\alpha = \sqrt{2(d-1)(d-2)}$. **Right panel:** $\alpha_{\mathcal{I}}^c > \alpha_{\mathcal{T}}^c$. In the overlap of red and blue regions ($\alpha_{\mathcal{T}}^c < |\alpha| < \alpha_{\mathcal{I}}^c$), either Kasner transition or inversion description breaks down.

Numerical verification:

Consider a 5-dimensional model:

$$\mathcal{L}^{(5)} = -\frac{1}{2}(\partial_\mu\psi)^2 - \frac{\sinh^2(\kappa\psi/2)}{2} \left(\partial_\mu\theta - \frac{\sqrt{3}}{L}A_\mu \right)^2 + \frac{3}{L^2} \cosh^2 \frac{\psi}{2} (5 - \cosh\psi) - \frac{1}{4}F_{\mu\nu}F^{\mu\nu},$$

At the AdS boundary:

$$\psi = \psi_s z + \dots + \psi_v z^3 + \dots, \quad A_t = \mu + \dots - \frac{\rho}{2} z^2 + \dots,$$

Kasner inversion: $\alpha\alpha_I = 12.$

Kasner transition: $\alpha + \alpha_T = \pm \frac{12}{|\kappa|},$

here “+” for positive alpha
while “-” for negative alpha

α - κ phase diagram

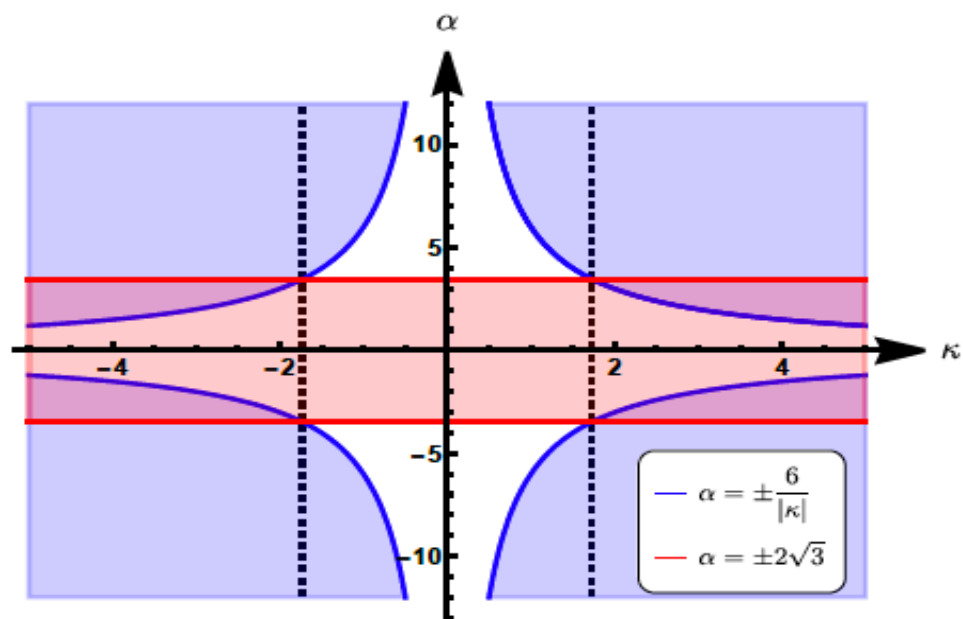


Figure 2: The κ - α phase diagram for the benchmark model (3.26). The two vertical dashed lines at $\kappa = \pm\sqrt{3}$ divide the phase diagram into three parts. The middle part with $-\sqrt{3} < \kappa < \sqrt{3}$ corresponds to **Case I**, and the outer parts $|\kappa| > \sqrt{3}$ correspond to **Case III**. In addition, **Case II** is precisely given by the two vertical lines.

1) The case of $\kappa = 2$ (This model ($\kappa = 2 > \sqrt{3}$) belongs to Case III.)

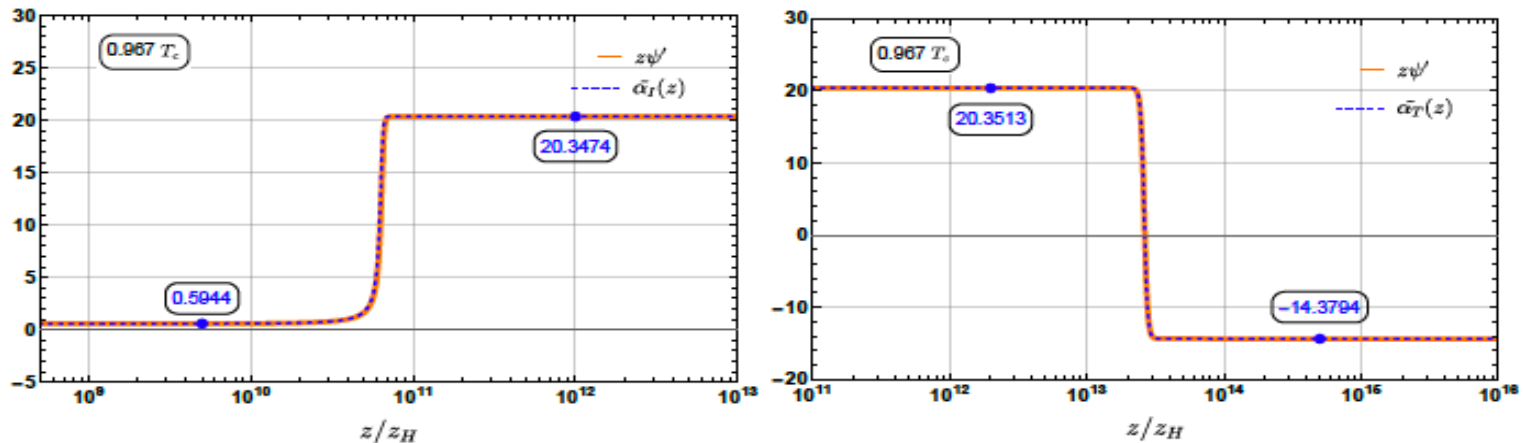


Figure 3: A direct comparison of the analytical description (3.30) (blue dashed curve) and the numerical one (solid orange curve) for **Kasner inversion** (left panel) and **Kasner transition** (right panel). Note from (3.11) that $\tilde{\alpha}(z) = z\psi'(z)$. Each platform corresponds to a Kasner epoch with the number denoting the value of α . We consider the hairy black hole at $T = 0.967T_c$. The approximation (3.30) is in excellent agreement to the profile from the full equations of motion (2.3)-(2.6). We have considered the model (3.26) with $\kappa = 2$, *i.e.* a top-down theory from supergravity [32].

Note that there is an overlapping region: $3 < |\alpha| < 2\sqrt{3}$.

Outside the overlapping region, the alternation between adjacent Kasner epochs is described by the transformation laws. Inside the overlapping region, however...

Here is the case for $T=0.995T_c$. After the ER collapse and scalar oscillation, one has a Kasner epoch with $\alpha=1.3078$, then after a Kasner inversion and a transition, the resulting epoch has $\alpha=-3.1966$ which is within the overlapping region: $(-2\sqrt{3}, -3)$.

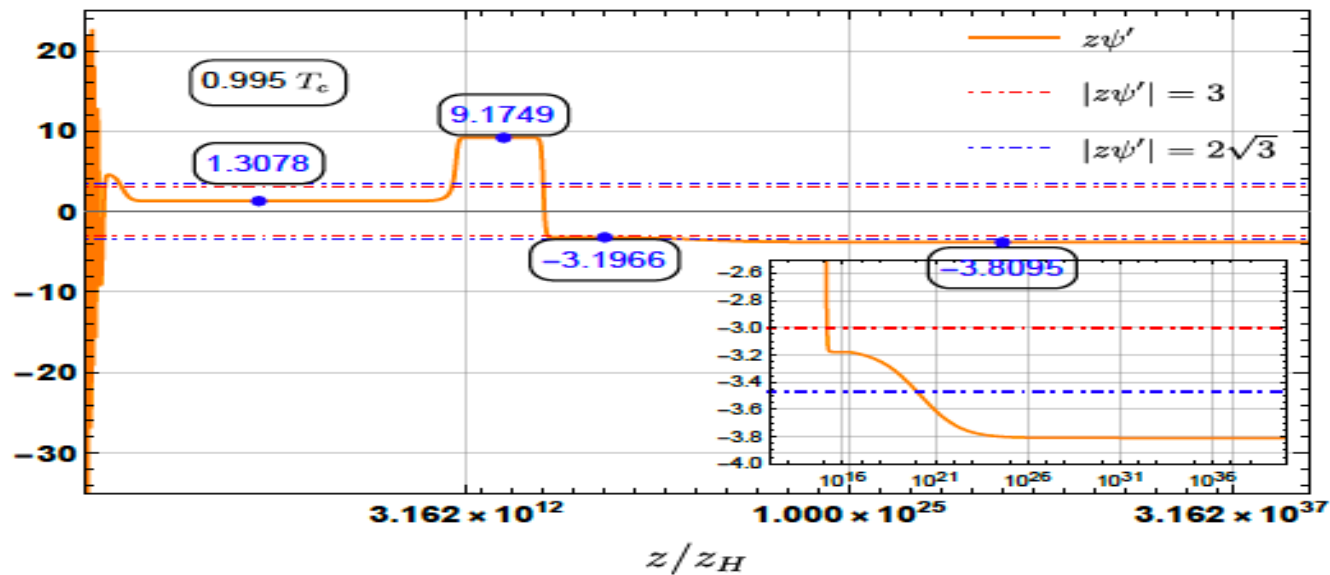


Figure 4: The configuration of $z\psi'$ inside the hairy black hole at $T = 0.995T_c$ for the model (3.26) with $\kappa = 2$. The dashed red and blue curves mark $|z\psi'| = 3$ and $|z\psi'| = 2\sqrt{3}$, respectively. The value of α for each Kasner epoch is given explicitly. When $z\psi' = -3.1966 \in (-2\sqrt{3}, -3)$, it goes through a competitive process that can't be described by our inversion or transition law. The inset zooms in on this transformation. After this process, the system arrives at a Kasner epoch with $\alpha = -3.8095$. The present model can be embedded into supergravity [32].

2) The case of $\kappa = \sqrt{3}$ (belongs to Case II)

There will be generically a never-ending chaotic alternation of Kasner epochs towards the singularity.

$$\begin{aligned} \alpha\alpha_I &= 12, & |\alpha| < 2\sqrt{3}, \\ \alpha + \alpha_T &= \pm 4\sqrt{3}, & |\alpha| > 2\sqrt{3}. \end{aligned}$$

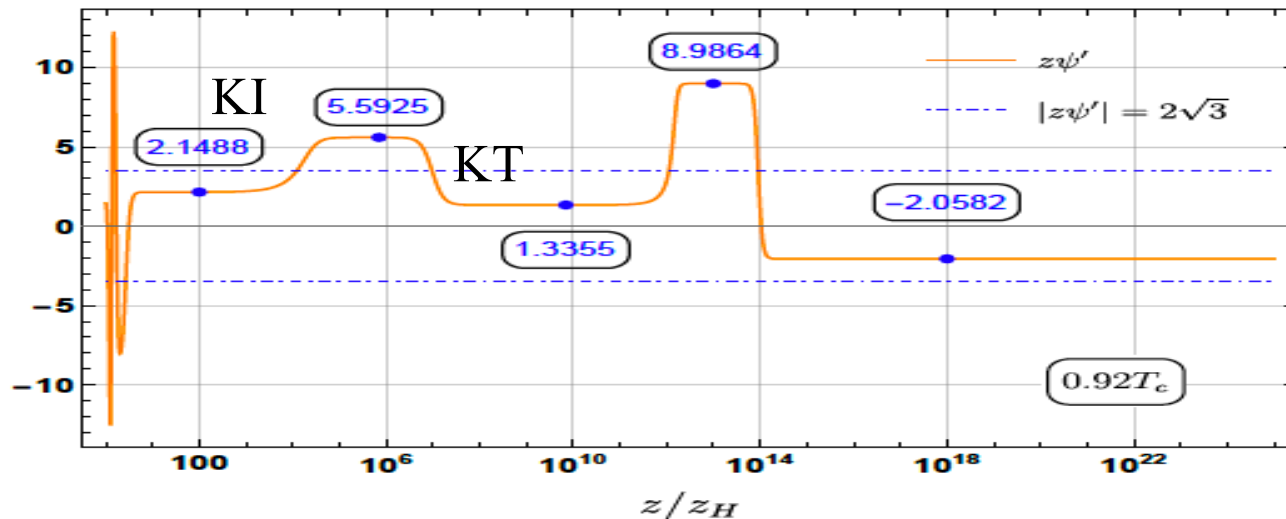


Figure 5: The interior configuration of $z\psi'$ at $T = 0.92T_c$ for the model (3.26) with $\kappa = \sqrt{3}$. Both the boundaries of the Kasner inversion and transition are at $|\alpha| = 2\sqrt{3}$, so it will be an infinite Kasner alternation process. The value of α for each Kasner epoch is given by solving the full equations of motion. The validity of the transformation rule (3.32) for the alternation of Kasner epochs is manifest.

3) The case of $\kappa = 3/2$ (belongs to Case I)

In this case there exists a stable region: $2\sqrt{3} < |\alpha| < 4$

Once a Kasner epoch falls into this region, it will stay at this Kasner epoch towards the singularity: After a Kasner transition around $z/z_H = 10^5$, the system jumps to a Kasner epoch with $\alpha = 3.6147$ within the stable region.

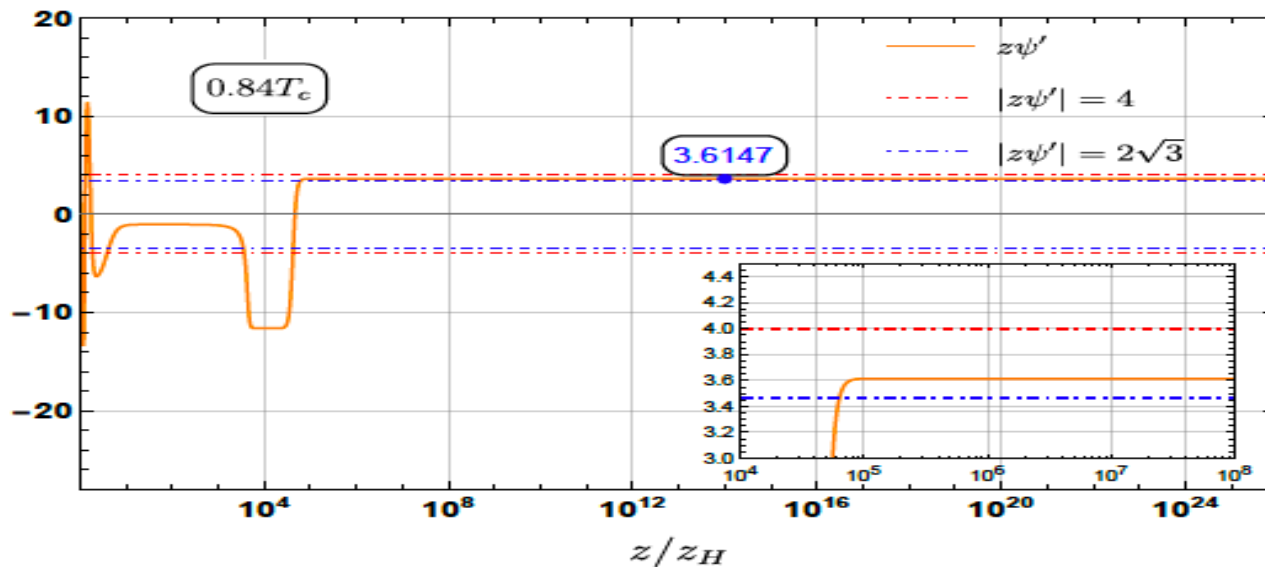


Figure 6: The interior profile for $z\psi'$ for the model (3.26) with $\kappa = 3/2$ and $T = 0.84T_c$. There is a stable region with $2\sqrt{3} < |\alpha| < 4$. One finds a stable Kasner epoch with $\alpha = 3.6147$ for $z/z_H > 10^5$. The inset zooms in on the transition.

The case with general coupling \mathcal{F} , while V neglected

Consider a 5-dimensional model with $\mathcal{F} = \sinh(\sinh^2(\psi))$, $V = -12 - \frac{3}{2}\psi^2$, $q = \sqrt{3}$.



$$\alpha' \simeq -\frac{h'}{h}\alpha - \frac{3A_t^2}{z^7 h^2} \frac{d\mathcal{F}}{d\psi},$$

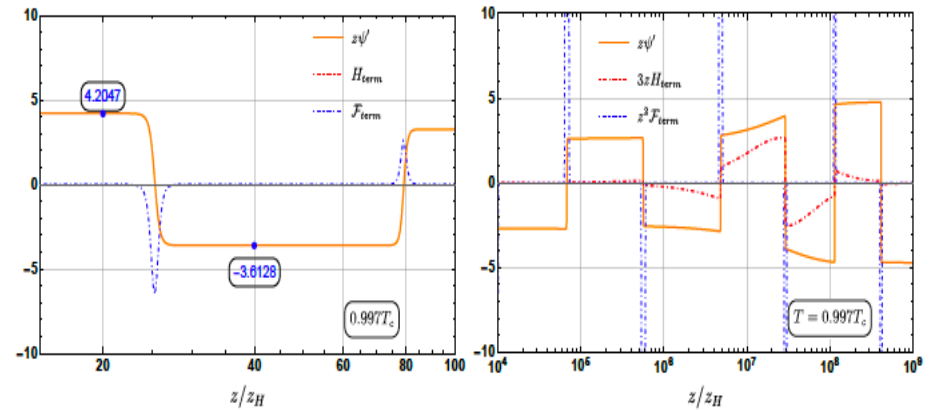
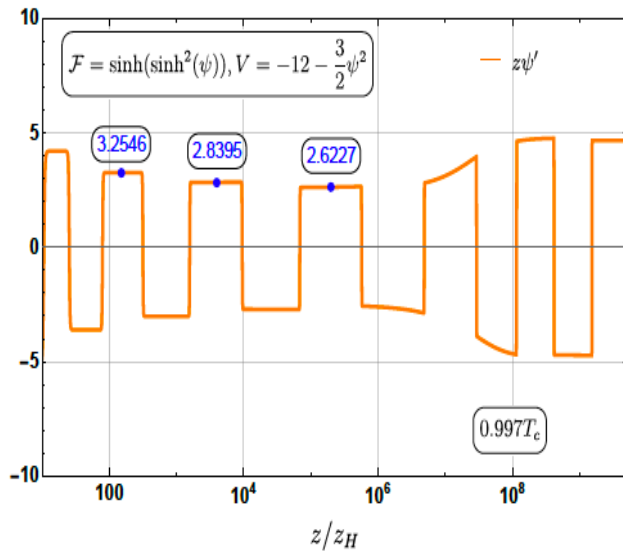


Figure 8: Zoom in on the evolution of $z\psi'$ in Fig. 7. The interior behavior is dominated by the two terms in the right hand of (4.4), for which the first term $\mathcal{H}_{\text{term}} = -\frac{h'}{h}\alpha$ is denoted by the red dashed curve and the second term $\mathcal{F}_{\text{term}} = -\frac{3A_t^2}{z^7 h^2} \frac{d\mathcal{F}}{d\psi}$ is denoted by the blue dashed curve. The left panel shows two Kasner transformations dominated by $\mathcal{F}_{\text{term}}$. When $10^6 < z/z_H < 10^8$, in the right panel non-Kasner epochs are manifest where both terms come into play.

The case with general potential V

When the scalar potential dominates

$$\psi'' = -\frac{1}{z}\psi' + \frac{e^{-\chi/2}}{z^{d+2}h} \frac{dV}{d\psi}, \quad \tilde{\alpha}' = \frac{e^{-\chi/2}}{z^{d+1}h} \frac{dV}{d\psi} \Rightarrow \tilde{\alpha}' \frac{dV}{d\psi} = \frac{e^{-\chi/2}}{z^{d+1}h} \left(\frac{dV}{d\psi} \right)^2 < 0,$$

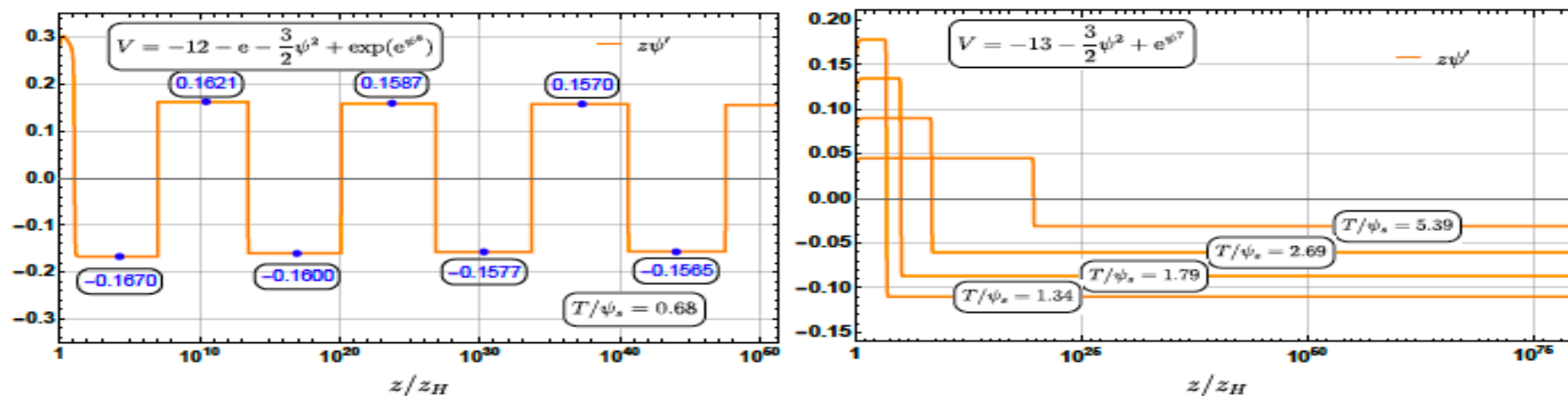


Figure 9: Kasner structure and transformation triggered by super-exponential potentials for the Einstein-scalar theory. The left panel is dominated by an even super-exponential potential $V \sim \exp(e^{\psi^8})$ and the right one is dominated by $V \sim e^{\psi^7}$. To highlight the role of scalar potential, we turn off the $U(1)$ gauge field. The scalar potentials are chosen to have the asymptotic behavior as $\psi \rightarrow 0$ near the AdS boundary $V = -12 - \frac{3}{2}\psi^2 + \dots$, for which the boundary expansion is given by (3.27). To obtain the hairy black holes in such charged neutral case, we fix the boundary source for the scalar $\psi_s = 1$. We consider the planar horizon case in five dimensional spacetime.

The case with both F and V

$$V(\psi) = -13 - \frac{3}{2}\psi^2 + e^{\psi^4}, \quad \mathcal{F} = \sinh^2(\psi), \quad q = \sqrt{3}.$$

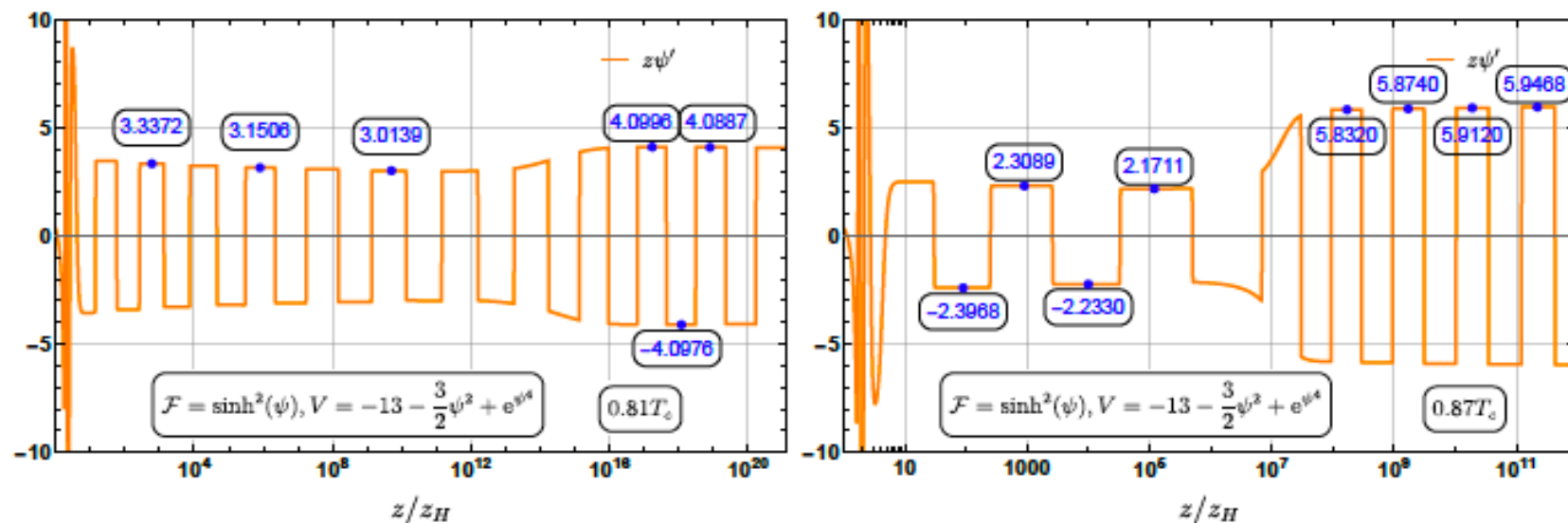


Figure 11: Interior dynamics of the planar hairy black holes at $T = 0.81T_c$ (left) and $T = 0.87T_c$ (right) for the model (4.7). There develop complicated behaviors, including the presence of non-Kasner epochs and the random change of the amplitude of the Kasner exponent.

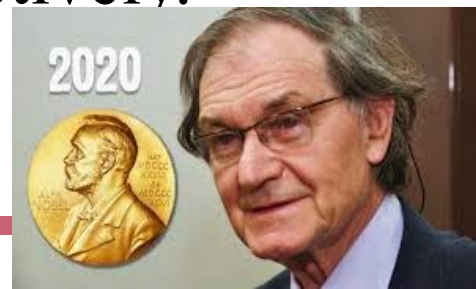
5. Constraining the number of horizons with energy condition

Einstein's equation in $(d + 1)$ dimensional spacetime $G_{\mu\nu} = \hat{T}_{\mu\nu}$

In the classical level the matter should satisfy some constraints named “**energy conditions**” which crudely describe **properties common to all** (or almost all) states of matter that are well-established in physics but are **sufficiently strong to rule out many unphysical “solutions”** of the Einstein's equation.

The original singularity theorems of Penrose and Hawking were proved for matter obeying the null energy condition (NEC) or **strong energy condition** (SEC), respectively.

$$[\hat{T}_{\mu\nu} - \hat{T}g_{\mu\nu}/(d - 1)]v^\mu v^\nu \geq 0 \quad \text{for every timelike vector field } v^\mu$$



5. Constraining the number of horizons with energy condition

Denote Γ to be the cross-section of black hole event horizon and ξ^μ to be the Killing vector which presents the static symmetry. We prove the following theorem for a static $(d + 1)$ -dimensional black hole.

Theorem 1 *If the Einstein's equation and one of the following three conditions are satisfied*

- (C1) Γ is compact and SEC is satisfied inside black hole;*
- (C2) Γ is noncompact but the system has hyperbolical or planar symmetry, and NEC is satisfied inside black hole;*
- (C3) Γ is noncompact 2-dimensional surface with nonpositive area-averaged scalar curvature, and NEC is satisfied inside black hole,*

then there is at most one non-degenerated inner Killing horizon associated with ξ^μ inside every connected branch of black hole event horizon. In addition, if a connected branch of black hole event horizon is degenerated, then there is no inner Killing horizon associated with ξ^μ .

Here we define the “area-averaged scalar curvature” of a surface S to be $\mathcal{A}^{-1} \int_S \mathfrak{R} dS$ with \mathcal{A} and \mathfrak{R} the area and scalar curvature of S , respectively.

Proof of C1:

Assume that behind the event horizon there is an connected spacetime region V inside which the Killing vector ξ is timelike

$$ds^2 = -N^2 dt^2 + h_{ab} dx^a dx^b$$

Einstein's equation:

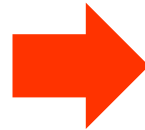
$${}^{(d)}R = 2\hat{\rho}, \quad \hat{\rho} = N^{-2} \hat{T}_{\mu\nu} \xi^\mu \xi^\nu$$

$${}^{(d)}R_{ab} = N^{-1} D_a D_b N + \left[\hat{T}_{ab} + \frac{h_{ab}}{d-1} (\hat{\rho} - \hat{T}) \right]$$

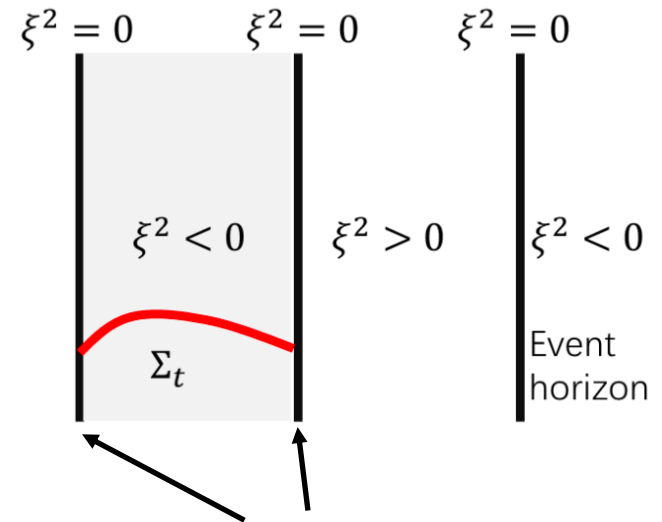


$$D^2 N^2 = 2N^2 [\hat{\rho} + \hat{T}/(d-1)] + 2h^{ab} (\partial_a N) (\partial_b N)$$

SEC: $\hat{\rho} + \hat{T}/(d-1) \geq 0.$



$$D^2 N^2 \geq 0$$



Maximum Principle: the maximum of N^2 must be at the boundaries:

$$\max N^2|_{\Sigma_t} = \max N^2|_{\partial\Sigma_t} = 0$$

which is contradictory to the assumption that ξ is timelike !

For the stationary case:

In an axisymmetric stationary spacetime, there are two linear independent Killing vectors, ξ^μ is timelike outside EH, and a spacelike vector field, Ψ^μ , representing the rotating symmetry.

$$ds^2 = -N^2 dt^2 + \gamma^2 (d\phi - \omega dt)^2 + q_{AB} dx^A dx^B$$

On the EH:

$$-N^2|_H = \frac{g_{tt}g_{\phi\phi} - g_{t\phi}^2}{g_{\phi\phi}} \Big|_H = 0.$$

Let us assume that: (A) there are more than two inner Killing horizons when EH is nongenerated, or (B) there is an inner Killing horizon when the EH is degenerated. Then there must be a spacetime region V , where the $N^2 > 0$ inside V and $N = 0$ at ∂V .

One can make an ADM decomposition on the spacetime V by a series of equal- t surface denoted by Σ_t . The induced metric

$$ds_{\Sigma_t}^2 = h_{ab} dx^a dx^b = \gamma^2 d\phi^2 + q_{AB} dx^A dx^B$$

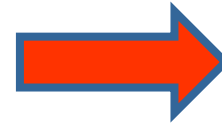
Then the Hamiltonian constraint and the momentum constraint:

$$\begin{aligned} {}^{(d)}R + K^2 - K_{ab}K^{ab} &= 2\hat{\rho}, \\ D^a K_{ab} - D_b K &= -\hat{J}_b \end{aligned}$$

On the other hand,

due to stationary, the evolution equation of extrinsic curvature and induced metric read

$$\partial_t K_{ab} = \partial_t h_{ab} = 0.$$



$${}^{(d)}R_{ab} - 2K_{ac}K^c_b = \frac{1}{N}\mathcal{L}_\beta K_{ab} + N^{-1}D_a D_b N + \left[\hat{\mathcal{T}}_{ab} + \frac{h_{ab}}{d-1}(\hat{\rho} - \hat{\mathcal{T}}) \right]$$

$$2NK_{ab} + \mathcal{L}_\beta h_{ab} = 0.$$

Here $\beta^a = -\omega\Psi^a$ is the shift vector field.

With the equations of motion, we are able to show

$$D^2N^2 = 2N^2[\hat{\rho} + \hat{T}/(d-1)] + 2h^{ab}(\partial_a N)(\partial_b N) + 2N^2K_{ab}K^{ab}.$$

Then we see that inside Σ_t with the SED, $\hat{\rho} + \hat{T}/(d-1) \geq 0$.

$$D^2N^2 \geq 0.$$

As the cross-section of horizons is compact, the domain Σ_t is bounded. The maximum principle shows that the maximum of N^2 must be at the boundaries of Σ_t , so we have

$$\max N^2|_{\Sigma_t} = \max N^2|_{\partial\Sigma_t} = 0,$$

which is contradictory to fact that $N^2 > 0$ inside Σ_t . This shows that the assumption (A) and (B) are wrong.

6. Conclusions

- We establish a no inner-horizon theorem for black holes with charged scalar hair.
- The hairy black holes approach a spacelike singularity at late interior time, independent of the form of scalar potentials and the asymptotic boundary of spacetimes.
- The geometry near the singularity takes a universal Kasner form when the kinetic term of the scalar hair dominates, while novel behaviors different from Kasner form are uncovered when the scalar potential becomes important to the background.
- All these features are also valid for the Einstein gravity coupled with neutral scalars.
- No Cauchy horizon for (charged) black holes with vector hairs, including GB case. Some interesting features appear inside the black holes, for example, never-ending Kasner epochs.
- We try a classification of the interior structure of black holes with scalar hairs, and the transformation laws for Kasner inversion and Kasner transition are presented.
- With quite general conditions, we find that the number of horizons is highly constrained by energy conditions of matter.

thanks!